The Effect of Radial Growth Rate on Wood Anatomical, Physical, and Mechanical Properties of the 26-Year-Old Sentang Tree (*Azadirachta Excelsa* (Jack) Jacobs) Planted in Jeli, Kelantan, Malaysia

by

MOHAMAD HAAZIQ BIN AHMAD

A thesis submitted in the fulfillment of the requirements for the degree of Master of Science (Forest Resources Technology)

FACULTY OF BIOENGINEERING AND TECHNOLOGY
UNIVERSITI MALAYSIA KELANTAN
2025

THESIS DECLARATION

I hereby certify that the work embodied in this thesis is the result of the original research and has not been submitted for a higher degree to any other University or Institution.

☐	**OPEN ACCESS**	I agree that my thesis is to be made immediately available as hardcopy or on-line open access (full text).
☐	**EMBARGOES**	I agree that my thesis is to be made available as hardcopy or on-line (full text) for a period approved by Post Graduate Committee. Dated from _____________until _____________
☐	**CONFIDENTIAL**	(Contains confidential information under the Official Secret Act 1972)*
☐	**RESTRICTED**	(Contains restricted information as specified by the organization where research was done)*

I acknowledge that Universiti Malaysia Kelantan reserves the right as follows.

1. The thesis is the property of Universiti Malaysia Kelantan.
2. The library of Universiti Malaysia Kelantan has the right to make copies for the purpose of research only.
3. The library has the right to make copies of the thesis for academic exchange.

_______________ SIGNATURE

_______________ SIGNATURE OF SUPERVISOR

_______________ IC/PASSPORT NUMBER
Date:

_______________ NAME OF SUPERVISOR
Date:

Note: * If the thesis is CONFIDENTIAL OR RESTRICTED, please attach the letter from the organization stating the period and reasons for confidentiality and restrictioN

ABSTRACT

It is widely accepted that in any given stand, the radial growth rate of the individual tree varies according to age, relationships with neighboring trees, and local site factors. Thus, even in the same site, each tree would exhibit different radial growth rates, which could affect the properties of the wood. In this regard, this study was conducted to investigate the properties of sentang wood and focused on examining the effect of radial growth rate on the anatomical, physical, and mechanical properties variations in the radial and longitudinal directions of the tree. Studying these properties is vital, as they are essential indicators for wood used in furniture, pulp, and wood-based composite production and are crucial determinants of suitability for structural applications. For these purposes, tree inventory was conducted on a 4.0 ha sentang site in Jeli, Kelantan, Malaysia using a 1.0 ha circular plot containing approximately 300 sentang trees, and 30 trees were randomly selected from this population. The trees were categorized into slow-, average-, and fast-growth based on their breast height diameter (DBH). The wood properties were then examined, including the fiber and vessel dimensions, moisture content (MC), density, shrinkage, and bending and compression strength along the radial and longitudinal directions of the trees. The results revealed that despite the differences in the radial growth rate, radial variation in the vessel element dimensions, air-dry density, MOR, MOE, and compression strength tend to have a typical pattern, experiencing an increase from the pith to the bark. In comparison, radial variation in the fiber dimensions, green density, and shrinkage were found to have varied patterns depending on the radial growth rate and longitudinal position. On the other hand, longitudinal variation in the fiber and vessel element dimensions tended to have varied patterns depending on the radial growth rate and radial position. Regarding the physical properties, except for the shrinkage, longitudinal variation in the MC and density was found to have a typical pattern despite the differences in the radial growth rate. The green MC experiences a decrease from the bottom to the top, while the density tends to increase toward the top of the trees. Similarly, longitudinal variation in the mechanical properties tended to have a typical pattern of an increase toward the top of the trees despite the differences in the radial growth rate. In addition, the radial growth rate seems to affect the wood properties in general. The slow-growth tree tends to have a shorter fiber length and smaller fiber diameter, reflecting a considerably higher wood density, and thus has the highest mechanical properties. In contrast, the fast-growth tree tends to have a lower wood density and thus has the lowest mechanical properties than the other categorized trees. The anatomical properties examination results revealed that the average fiber length and diameter of the slow-,

average- and fast-growth trees were 833 and 16.6, 964 and 21.9, and 927 and 20.7 µm, respectively. Additionally, the average vessel element length and diameter of the slow-, average- and fast-growth trees were 618 and 390, 576 and 328, and 550 and 369 µm, respectively. Regarding the physical properties, the average green MC of the slow-, average- and fast-growth trees were 42.0, 39.3, and 48.4%, respectively. The average green and air-dry wood density of the slow-, average- and fast-growth trees were 689 and 567, 699 and 587, and 679 and 550 kg/m^3, respectively. The shrinkage in the tangential direction of the slow-, average- and fast-growth trees were 3.03, 3.19, and 3.85%, respectively. The shrinkage in the radial direction of the slow-, average- and fast-growth trees were 1.83, 1.79, and 2.41%, respectively. The shrinkage in the longitudinal direction of the slow-, average- and fast-growth trees were 0.53, 0.61, and 0.82%, respectively. In the case of mechanical properties, the average MOR and MOE of the slow-, average- and fast-growth trees were 85.2 and 8,811, 84.4 and 8,043, and 79.3 and 8,314 N/mm^2, respectively. In addition, the compression strength of the slow-, average- and fast-growth trees were 36.3, 35.9, and 34.0 N/mm^2, respectively.

ABSTRAK

Secara umumnya, di mana-mana dirian hutan, kadar pertumbuhan jejari bagi setiap individu pokok akan berbeza mengikut umur, hubungan dengan pokok terdekat, dan faktor tapak. Justeru, walaupun tumbuh di tapak yang sama, setiap pokok akan mempunyai kadar pertumbuhan jejari yang berbeza, yang boleh mempengaruhi sifat kayu. Dalam konteks ini, kajian ini dijalankan untuk menyelidik sifat kayu sentang dimana fokusnya adalah kesan kadar pertumbuhan jejari terhadap variasi dalam sifat anatomi, fizik dan mekanik kayu pada arah jejari dan membujur pokok. Kajian ini adalah penting sebagai penunjuk bagi kesesuaian kayu untuk penghasilan perabot, pulpa, komposit kayu, dan kayu untuk struktur binaan. Untuk tujuan ini, inventori pokok dijalankan di tapak sentang seluas 4.0 ha di Jeli, Kelantan, Malaysia menggunakan plot bulat seluas 1.0 ha yang mengandungi kira-kira 300 pokok sentang, dan 30 pokok dipilih secara rawak daripada populasi ini. Pokok sentang kemudian dikategorikan kepada tiga kadar pertumbuhan jejari, yaitu kadar pertumbuhan perlahan, sederhana dan pantas berdasarkan diameter pokok pada paras dada (DBH). Dimensi gentian dan unsur vesel, kandungan lembapan, ketumpatan, pengecutan, dan kekuatan lentur dan mampatan kayu kemudian diukur. Hasil pengukuran menunjukan bahwa walaupun kadar pertumbuhan jejari berbeza, variasi pada arah jejari pokok untuk dimensi unsur vesel, ketumpatan kering udara, MOR, MOE, dan kekuatan mampatan mempunyai corak yang sama, yaitu cenderung meningkat dari empulur menuju kulit kayu. Sebagai perbandingan, variasi untuk dimensi gentian, ketumpatan basah, dan pengecutan mempunyai corak yang berlainan, bergantung pada kadar pertumbuhan jejari pokok dan kedudukan membujurnya. Sebaliknya, variasi pada arah membujur pokok untuk dimensi gentian dan unsur vesel mempunyai corak yang berlainan, bergantung pada kadar pertumbuhan jejari pokok dan kedudukan jejarinya. Untuk sifat fizik kayu, kecuali pengecutan, variasi untuk kandungan lembapan dan ketumpatan kayu mempunyai corak yang tipikal walaupun kadar pertumbuhan jejari pokok berbeza, yaitu kandungan lembapan cenderung menurun menuju bahagian atas pokok, sebaliknya ketumpatan cenderung meningkat menuju bahagian atas pokok. Begitu juga variasi untuk MOR, MOE dan kekuatan mampatan kayu, mempunyai corak yang sama, yaitu cenderung meningkat menuju bahagian atas pokok. Selain itu, kadar pertumbuhan jejari pokok juga terlihat berpengaruh pada sifat kayu secara umumnya. Pokok dengan kadar pertumbuhan jejari perlahan cenderung mempunyai panjang gentian yang lebih pendek dan diameter gentian yang lebih kecil, mencerminkan ketumpatan dan sifat mekanikal yang paling tinggi. Sebaliknya, pokok dengan kadar pertumbuhan jejari pantas cenderung mempunyai ketumpatan dan sifat mekanikal yang

paling rendah. Keputusan pemeriksaan sifat anatomi kayu mendedahkan bahawa purata panjang gentian dan diameter bagi pokok dengan kadar pertumbuhan jejari perlahan, sederhana dan pantas adalah masing-masing 833 dan 16.6, 964 dan 21.9, dan 927 dan 20.7 µm. Di samping itu, purata panjang dan diameter unsur vesel untuk pokok dengan kadar pertumbuhan jejari perlahan, sederhana dan pantas ialah masing-masing 618 dan 390, 576 dan 328, dan 550 dan 369 µm. Mengenai sifat fizik kayu, purata kandungan lembapan basah bagi pokok dengan kadar pertumbuhan jejari perlahan, sederhana dan pantas adalah masing-masing 42.0, 39.3, dan 48.4%. Purata ketumpatan kayu basah dan kering udara untuk pokok dengan kadar pertumbuhan jejari perlahan, sederhana dan pantas adalah masing-masing 689 dan 567, 699 dan 587, dan 679 dan 550 kg/m^3. Pengecutan kayu pada arah tangensial bagi pokok dengan kadar pertumbuhan jejari perlahan, sederhana dan pantas ialah masing-masing 3.03, 3.19, dan 3.85%. Pengecutan kayu pada arah jejari bagi pokok dengan kadar pertumbuhan jejari perlahan, sederhana dan pantas ialah masing-masing 1.83, 1.79, dan 2.41%. Selain itu, pengecutan kayu pada arah membujur bagi pokok dengan kadar pertumbuhan jejari perlahan, sederhana dan pantas ialah masing-masing 0.53, 0.61, dan 0.82%. Dalam kes sifat mekanik kayu, purata MOR dan MOE bagi pokok dengan kadar pertumbuhan jejari perlahan, sederhana dan pantas adalah masing-masing 85.2 dan 8,811, 84.4 dan 8,043, dan 79.3 dan 8,314 N/mm^2. Di samping itu, kekuatan mampatan kayu untuk pokok dengan kadar pertumbuhan jejari perlahan, sederhana dan pantas adalah masing-masing 36.3, 35.9, dan 34.0 N/mm^2.

ACKNOWLEDGEMENTS

In the name of Allah, the Most Merciful and the Most Gracious. All praise to Allah. He knows whatever goes into the earth and whatever comes out of it, and whatever descends from the sky and whatever ascends into it. And He is the Most Merciful, All-Forgiving. All praise to Allah. He taught human beings what they did not know. May the peace and blessings of Allah be upon Prophet Muhammad, his family, and all his companions. I want to express my sincere gratitude to my mother, Wan Zubaidah binti Wan Mohamad, and my father, Ahmad bin Ibrahim. Thank you for your prayers, endless love, support, and care. I want to thank my supervisor, Dr. Andi Hermawan, and my co-supervisor, Assoc. Prof. Ts. Dr. Mohd Hazim bin Mohamad Amini and Ts. Dr. Sharizal bin Ahmad Sobri, lab staff, and colleagues for their valuable guidance and help during my study. I am also grateful to the Ministry of Higher Education for financial assistance under the Fundamental Research Grant Scheme (FRGS/1/2019/WAB07/UMK/02/1

LIST OF TABLES

LIST OF FIGURES

LIST OF ABBREVIATIONS

DBH	Diameter at Breast Height
EMC	Equilibrium Moisture Content
FAO	Food and Agriculture Organization
FDPM	Forestry Department of Peninsular Malaysia
FPDSB	Forest Plantation Development Sdn. Bhd.
FRIM	Forest Research Institute Malaysia
FSP	Fiber Saturation Point
GBIF	Global Biodiversity Information Facility
MC	Moisture content
MDF	Medium density fiberboard
MOE	Modulus of elasticity
MOR	Modulus of rupture
MTIB	Malaysian Timber Industry Board
PRF	Permanent Reserved Forest
OD	Oven-dry
SD	Standard deviation
SEM	Scanning electron microscopic
UTM	Universal testing machine

LIST OF SYMBOLS

kg/m^3	Kilogram per cubic meter
ha	Hectare
%	Percentage
N/mm^2	Newton per square millimeter
cm	Centi meter
m^3	Cubic meter
m	Meter
N	North
E	East
d_{av}	Average DBH
DBH_{sg}	DBH of slow-growth tree
DBH_{ag}	DBH of average-growth tree
DBH_{fg}	DBH of fast-growth tree
L_f	Fiber length
L_v	Vessel element length
d_f	Fiber diameter
d_v	Vessel element diameter

°C	Degree Celsius
αM	Shrinkage at M% MC
l_0	Dimension at green MC
l_M	Dimension at M% MC
h	Hour
m_1	Green mass
m_0	Mass after oven-dry
P	Maximum load
P_1	Load at the limit of proportionality
N	Newton
L	Span length
b	Width
h	Thickness
d_1	Deflection at the limit of proportionality
mm/min	Millimeter per minute
mm	Millimeter
F	Compression strength
A	Cross section area

TABLE OF CONTENT

INTRODUCTION

1.1 Background

Forest plantations are generally established to secure the long-term supply of raw materials for wood-based industrial and non-industrial purposes. It is widely recognized that forest plantations are usually designated as an essential source of wood supply due to their markedly faster growth rate and, thus, higher wood yield than natural forests. Hence, the primary reason for establishing forest plantations was to ease the natural forest burden by providing the woods for industrial purposes, such as sawn timbers and pulpwood, and non-industrial purposes, including soil protection and fuelwood for local communities (Carle et al., 2002; Gunter et al., 2011).

In Malaysia, several fast-growing species, such as rubberwood (*Hevea brasiliensis*) and acacia (*Acacia mangium*), have been used to establish a large-scale industrial forest plantation owned by private sector companies. Subsequently, the Malaysian government introduced additional fast-growing species for forest plantation establishment in the 1990s, one of which was sentang

(*Azadirachta excelsa* (Jack) Jacobs). Since then, the planting of sentang has been actively promoted, resulting in the establishment of numerous small-scale sentang plantations (Yahya & Weinland, 1995; FAO, 2002). In 2006, more than 8,000 ha of sentang plantation had already been established in Peninsular Malaysia, primarily in Kedah, Perak, Negeri Sembilan, Johor, and Pahang (Huat et al., 2003; Hashim et al., 2015).

Consequently, studies on sentang have been actively conducted, and several authors have documented the varying aspects of sentang in general. For example, some authors reported the morphological features of the tree, the gross macroscopic and workability of the wood, and its uses (Yahya & Mahat, 1998; Wong et al., 2002; Nordahlia et al., 2013). The other researcher reported rough anatomical, physical, mechanical, drying, and preservative treatability properties of the wood (Noraini, 1997; Trockenbrodt et al., 1999; Ruddin et al., 2020; Hermawan et al., 2020).

Sentang belongs to the Maleaeceae family, with a wood density range between 550–780 kg/m^3. The wood has solitary vessels or multiples of up to 5 or rarely more, commonly clustering up to 4–5 vessels. The vessel tends to be arranged in tangential and radial series of up to 4 vessels with a round to oval shape, sometimes filled with the deposition of dried extractives, especially in heartwood (Nordahlia et al., 2013). The wood is categorized as light-hardwood with shrinkage in the tangential and radial directions of 1.2 and 0.5%, respectively (Wong et al., 2002). The wood was reported to have good mechanical properties with the modulus of rupture (MOR), modulus of elasticity (MOE), and compression strength of 60, 6770, and 31 N/mm^2, respectively, and thus suitable for lightweight wooden construction purposes (Noraini, 1997). Other than that, massive information on the effectiveness of sentang extract for medicinal purposes was reported by several authors (Kurose et al., 2005; Kaewnang-O et al., 2011; Hummel et al., 2016).

On the other hand, more comprehensive studies have been conducted by some research groups to investigate the properties of sentang wood. However, these studies focused on the properties of the young-age sentang tree. For instance, a research group conducted extensive studies on the fiber morphology and physical and mechanical properties of 10-year-old sentang trees at the lower, middle, and upper portions of the trees grown with two different propagation techniques, including seedling and rooted cutting (Nordahlia et al., 2011; Nordahlia et al., 2014). The other researchers studied the physical properties of

10-year-old sentang trees planted in Sabah and the chemical properties of 8-year-old sentang trees planted in Malacca, Malaysia (Trockenbrodt et al., 1999; Rafeadah & Rahim, 2007). Meanwhile, a group of researchers outside Malaysia studied the effects of the radial growth rate on the properties of 4-year-old sentang trees planted in Indonesia (Wahyudi et al., 2016).

As stated above, previous studies were conducted to provide general information on the properties of sentang wood, and some authors focused more on the wood properties of young sentang trees. It is well known that the young age tree has different properties from the mature tree, and thus, the young age trees are generally harvested for fiber and chip resources, while the mature trees are harvested for their timber. Therefore, more samples from mature trees planted in different sites with different geographical and environmental characteristics must be studied to draw general conclusions regarding the properties of the wood.

In this regard, the current study focused on the effects of radial growth rate on the wood properties of the 26-year-old sentang trees planted in Jeli, Kelantan, Malaysia. The anatomical, physical, and mechanical properties variations of sentang wood in the radial and longitudinal directions of the trees were then examined.

1.2 Problem Statement

While planting acacia on a commercial scale was instituted in 1962, growing sentang on a plantation basis for commercial wood production is relatively new in Malaysia. Sentang has been recognized as a wood resource with significant potential value, primarily due to its extensive distribution and coverage and good wood quality, making it suitable for various applications.

On the other hand, within a given stand, the radial growth rate of the individual tree can vary significantly due to factors such as age, competition with neighboring trees, and local site conditions. A study in the Bukit Lagong Forest Reserve reported significant variations in radial growth rates within a 40-year-old sentang plantation where the average diameter of all trees was 34.9 cm, while the average diameter of 100 dominant trees was 51.8 cm (Yahya & Mahat, 1996). These significant variations in diameter suggest that the radial growth rate could substantially impact its wood properties, emphasizing the need to elucidate the influence of radial growth rate on the anatomical, physical, and mechanical properties of the wood.

Studying these properties is critical, as these properties are essential indicators for the suitability of the wood used in various applications, including furniture production, pulp and paper fabrication, and wood-based composites manufacturing, as well as crucial determinants of suitability for structural purposes. Despite the importance of this information, compared to other forest plantation species, only limited national information is available regarding the effect of the radial growth rate of sentang trees on the variation of wood properties in the radial and longitudinal directions of the tree. In addition, previous studies were conducted to provide general information on the properties of the wood, and some authors focused more on the wood properties of young sentang trees. It is well known that the young-age tree has different properties from the mature tree.

This research addresses the need for comprehensive data on the wood properties of mature sentang trees, especially those grown in different geographical and environmental conditions. By filling this gap, the study provides valuable insights that can enhance the utilization of sentang wood in commercial applications and improve the management of sentang plantations in Malaysia.

1.3 Objectives

The objectives of this study were as follows.

1. To examine the effect of radial growth rate on the anatomical properties variations in the radial and longitudinal directions of the 26-year-old sentang tree planted in Jeli, Kelantan, Malaysia.
2. To examine the effect of radial growth rate on the physical properties variations in the radial and longitudinal directions of the 26-year-old sentang tree planted in Jeli, Kelantan, Malaysia.
3. To examine the effect of radial growth rate on the mechanical properties variations in the radial and longitudinal directions of the 26-year-old sentang tree planted in Jeli, Kelantan, Malaysia.

1.4 Scope of Study

This study was carried out to investigate the effect of radial growth rate on the anatomical, physical, and mechanical properties variations in the radial and longitudinal directions of the 26-year-old sentang trees planted in Jeli, Kelantan, Malaysia. For these purposes, three trees categorized as slow-, average-, and fast-growth based on their breast height diameter (DBH) were harvested, and the anatomical properties variations in the radial and longitudinal directions of the trees, including variations in the fiber and vessel element dimensions, were examined. In addition, the effect of radial-growth rate on the physical properties variations in the radial and longitudinal directions of the trees, including variations in the green moisture content (MC) and density, air-dry density, and shrinkage in the tangential, radial, and longitudinal directions, were examined. Lastly, the effect of radial-growth rate on the mechanical properties variations in the radial and longitudinal directions of the trees, including variations in the bending strength and compression strength parallel to the fiber, were examined.

1.5 Significance of Study

This study was initiated to determine the extent of variation in wood properties of the 26-year-old sentang planted in Jeli, Kelantan, Malaysia. This study concerns the effect of radial growth rate on the variations in the fiber and vessel dimensions, MC, density, shrinkage, bending properties, and compression strength in the radial and longitudinal directions of the tree. As mentioned above, studying these properties is critical, as these properties are essential indicators for wood used in furniture, pulp, and wood-based composite applications, as well as crucial determinants of suitability for structural purposes. Therefore, the findings of this study could reveal the more significant potential of sentang for a broader range of end-products and assist the Malaysian government in optimizing wood production management from forest plantations.

CHAPTER 2

LITERATURE REVIEW

2.1 Forest in Peninsular Malaysia

In 2018, it was estimated that the forested land area in Peninsular Malaysia covered 5.76 million ha. This accounts for nearly half of the total land area in Malaysia, representing approximately 43.59% of the total 13.21 million ha (FDPM, 2018). Nevertheless, Figure 2.1 demonstrates an observable trend of declining forested land area in Peninsular Malaysia, accompanied by an annual increase in non-forested land area. The loss of forested land area may occur for many reasons, including deforestation, fire, and logging. Even so, the loss will eventually be gained in sustainably managed forests when young trees become large enough to achieve canopy closure (Atiqah, 2020).

In addition, out of 5.76 million ha of forested land area, 4.80 million ha have been gazetted as Permanent Reserved Forests (PRF) under the National Forestry Act 1984. The PRF serves multiple functions, including protecting soil, water, and ecosystem services, which are encompassed within the protection forest component. Additionally, the production forest component of the PRF is responsible for generating wood, fiber, bio-energy, and non-wood forest products. Table 2.1 summarizes the area of PRF by forest types in Peninsular Malaysia in 2007, 2010, 2015, and 2018, showing a consistent coverage area over time, indicating stability and continuity across successive years.

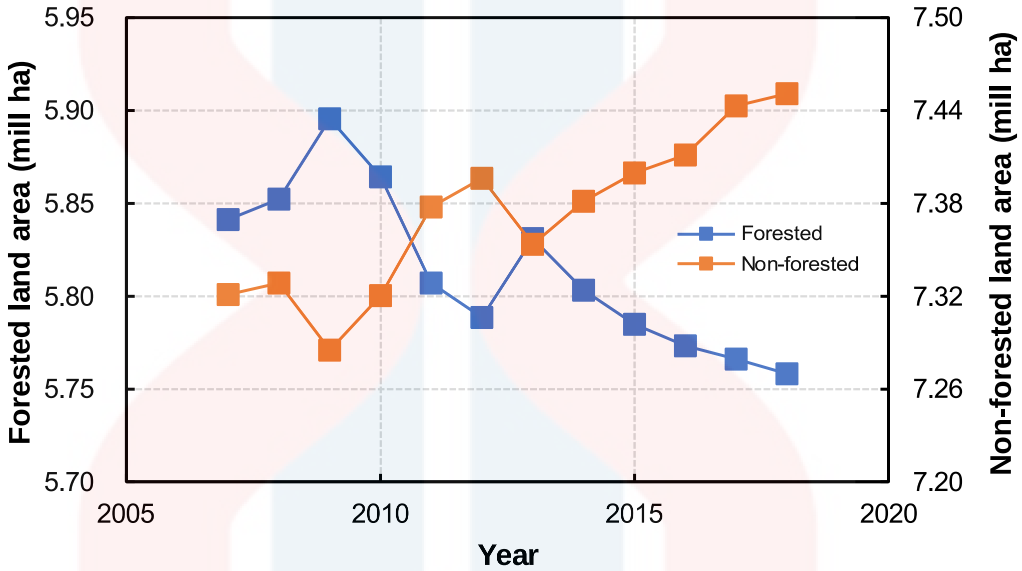

Sources: FDPM Annual Reports.

Figure 2.1: Fluctuations of forested and non-forested land areas in Peninsular Malaysia

Table 2.1: Area of PRF by forest types in Peninsular Malaysia.

PRF	Year			
	2007	2010	2015	2018
Natural forest (million ha)				
Inland forest	4.25	4.47	4.17	4.34
Peat swamp forest	0.24	0.24	0.25	0.25
Mangrove forest	0.10	0.10	0.11	0.09
Forest plantation (million ha)	0.10	0.11	0.39	0.12
Total (million ha)	4.69	4.92	4.92	4.80

Sources: FDPM Annual Reports

2.2 Forest Plantation

Generally, forest plantations are defined based on the planting or seeding of forest stands as a process of afforestation or reforestation. Usually, the forest plantation production systems involve a fast-growing monoculture or indigenous species. The selected species are planted in uniform-spaced rows, resulting in an even-age stand, and are treated using similar silvicultural practices throughout all the plantation areas (Evans, 1999; Kanowski, 2001; Carle et al., 2002).

It is well known that forest plantations are established to provide raw materials for industrial and non-industrial purposes. Therefore, forest plantations have already become an essential source of wood supply due to intensive forest management, resulting in a more rapid growth than natural forests. Forest plantations also offer non-wood forest products, including soil protection, carbon sequestration, clean water and air supply, land rehabilitation, job creation, and biodiversity conservation. Thus, it is believed that more natural forests might be protected if more forest plantations were well-established and managed (Carle et al., 2002; Zhang & Stanturf, 2008).

In addition, forest plantation development was influenced initially by wood market values, and thus, the primary reason for establishing forest plantations was also to generate a financial benefit. Moreover, some government policies in some countries have provided significant financial incentives to the private sector to participate in the forest plantation establishment program (Zhang & Stanturf, 2008). Therefore, the global forest plantation area has experienced a substantial increase, reaching 294 million ha, with an average annual growth rate of 1.85% since 1990. Notably, North and Central America, South America, and Asia have exhibited higher average annual increments of 2.51, 2.38, and 2.27%, respectively (FAO, 2020).

In Malaysia, forest plantation was introduced, followed by Japan, the United States, China, India, and the Russian Federation, as one strategy for overcoming the wood resource shortage and maintaining the expansion of downstream wood-based industries. It was reported that the Forest Research Institute Malaysia (FRIM) started a trial of forest plantation plots in the 1920s using various fast-growing species (Selvaraj & Muhammad,1980; FAO, 2002). However, the initial extensive commercial forest plantation arose with the projected establishment of pulp and paper mills in Peninsular Malaysia in 1967, employing fast-growing tropical pine and araucaria species (Freezailah & Fielding, 1971).

Since then, the Malaysian government has attempted to complement the log supply from the natural forest by establishing forest plantations. In 1990, the Malaysian government initiated a substantial commercial forest plantation development program using eight fast-growing species, including acacia, rubberwood, kelempayan, batai, sentang, khaya, binuang, and teak. In this initiative, the Ministry of Plantation Industries and Commodities assigned USD 250 million to be managed by the Malaysian Timber Industry Board (MTIB) over 15 years to establish 375,000 ha of forest plantations in Peninsular Malaysia by the year 2020 at a rate of 25,000 ha annually. However, a recent report estimated that the total area of forest plantations established in Peninsular Malaysia was 113,810 ha, of which rubberwood and other forest species covered 78,479 and 35,331 ha, respectively (FPDSB, 2018).

From the above results, it seems that the forest plantation establishment has still not fulfilled the target, with the forested area being far below the target. One of the primary obstacles encountered in establishing forest plantations is the limited availability of land. In most cases, the land designated for forest plantation establishment in Malaysia is situated in challenging and rugged terrains. Therefore, forest management activities, including silvicultural practices, may be hindered by relatively elevated expenses, resulting in less participation from the smaller players due to substantial capital investment costs (Ratnasingam, 2019). Additional obstacles in establishing forest plantations in Malaysia include soil quality, the management of pests and diseases, and the consistent availability of high-quality planting material. These factors continue to limit the long-term sustainability of forest plantations in the region (Ratnasingam et al., 2020).

2.3 Wood Supply from Forest Plantation

Table 2.2 displays recent data on log production originating from forest plantations in Malaysia. It is clear from the table that forest plantation in Peninsular Malaysia has a significant role in supplying domestic consumption with rubberwood as the major species. On the other hand, most of the wood extracted from forest plantations in Sabah and Sarawak was exported to East Asia and Indonesia as wood chips, designated as raw materials for biomass energy, pulp, and paper. Hence, the actual wood supply for domestic use from the forest plantations in Peninsular Malaysia was relatively smaller than initially expected (MTIB, 2019). In this regard, the capacity of forest plantations to alleviate the inadequate wood supply in the domestic market remains unsatisfactory. Thus, the capability of forest plantations in Malaysia to relieve the burden on wood supply from the natural forests is still constrained and could negatively affect the local wood-based industry.

Table 2.2: Log production in Malaysian forest plantations

Region	Wood volume output (m^3/year)	Total harvest area (ha/year)	The species composition (rubberwood to other species)	The ratio of export to domestic consumption
Peninsular Malaysia	1.5 million	15,000	85:15	18: 82
Sarawak	1.7 million	8,500	40:60	70:30
Sabah	600,000	3,000	45:55	65:35

Source: Ratnasingam et al. (2020) with modification

Out of some challenges in forest plantation establishment mentioned earlier, the situation above is probably because many tree species previously recommended for forest plantation establishment have not been carefully assessed, resulting in low performance and yield. Therefore, an extensive research network seems needed among the stakeholders, the private sector, government agencies, and universities to overcome this problem (Ratnasingam et al., 2020).

2.4 Sentang Tree

Sentang (*Azadirachta excelsa* (Jack) Jacobs) is a fast-growing indigenous species to Malaysia. Sentang is one of the species recommended by the Forestry Department of Peninsular Malaysia for forest plantation establishment due to its fast growth, thus having short rotation and time to harvest, resulting in a higher yield than other species from natural forests. Moreover, the fast-growing species usually are pioneers that can grow in marginal land with low content of topsoil (Adi et al., 2014).

2.4.1 Taxonomy and Ecology of Sentang Tree

Sentang belongs to the Maleaeceae family and is known as sentang, ranggu, and kayu bawang in Malaysia and Indonesia, neem in Phillipine, sa-dao-thiam in Thailand (Orwa et al., 2009). The Meliaceae family also includes species of significant economic importance to Malaysia, such as mahogany (*Swietenia* spp). The following is the taxonomy of sentang (Jacobs, 1961; GBIF, 2021).

Kingdom	:	Plantae
Class	:	Magnoliopsida
Order	:	Sapindales
Family	:	Meliaceae
Genus	:	Azadirachta
Specific Epithet	:	excelsa (Jack) Jacobs

It was reported that sentang is found in tropical dry, evergreen forests around the Malesian region, including Sumatera, Malaysia, Papua New Guinea, Thailand, and the Philippines (Mabberly & Pannell,1989; Kijkar, 1995; Yahya &

Mahat, 2002).

Source: Premono et al. (2019).

Figure 2.2: Sentang trees planted using an agroforestry system in Bengkulu, Indonesia

Sentang is a light-demanding tree well-grown in lowland forests with an elevation of 250 m and an average annual rainfall of 1600 mm (Kijkar, 1995). The tree grows in alluvial, medium-textured, free-draining, acidic soils. It also grows on clay, granite, lateritic, and limestone soils. However, the tree cannot tolerate waterlogging or frequent flooding. The tree flowering and fruiting are commonly about 6–7 years old, and bats disperse the seeds. The trees are planted along the sides of roads in the villages and as shade trees around the house. Sentang is also well-suited for agroforestry systems, which can be grown alongside other crops such as rubberwood, soybean, and other crops, as shown in Figure 2.2. This mixed-cropping system benefits from the leaf litter of sentang, which acts as a soil improver for agriculture (Orwa et al., 2009). Additionally, sentang trees exhibit higher growth rates than those in monoculture systems, likely due to the additional nutrients provided during fertilizing the accompanying crops (Rahmawathi et al., 2017). It was reported that sentang does not require careful care and is free from insect attacks because it produces a chemical substance called azadirachtin that can be used as an insecticide (Isman et al., 1990; Zhong et al., 2017; Bernardes et al., 2018).

In Kelantan, village names such as Wakaf Sentang, Kampung Sentang, and Madrasah Sentang are involved in the name of this tree with the community.

2.4.2 Morphology and Description of Sentang Tree

Sentang tree is a large deciduous tree growing up to 50 m tall. The straight, cylindrical bole can be free of branches up to 20 m, with a diameter of up to 125 cm, without buttresses (Yahya & Mahat, 1998).

The bark is pink or brownish grey, smooth when young, and becomes fissured and shaggy bark with grey, fibrous, oblong flakes in older trees. The tree has green compound leaves, an alternate arrangement, typically measuring around 30–75 cm long. Each leaf comprises approximately 7–11 pairs of asymmetric elliptic leaflets with 3–5 cm long and 2–3 cm wide. The flower is greenish-white fragrant and borne on axillary panicle inflorescences up to 70 cm long, with five white petals measuring about 0.5–0.65 cm long and 0.15–0.25 cm wide. The fruit is an oblong drupe, measuring approximately 2.5–3.5 cm long, turns green to yellow when ripened, and contains one seed (Mabberley et al., 1995; Kijkar & Boontawee, 1995).

2.4.3 Uses of Sentang Tree

Sentang wood is widely used for various end-products, including carving, raw material for medium-density fibreboard (MDF), veneer, particleboards, paneling, flooring, furniture, and musical instrument manufacturing, and lightweight construction such as house frames and boat building (Trockenbrodt et al., 1999; Wong et al., 2002). In addition, studies on the use of sentang as fillers in wood plastic composite (WPC) production have shown promising results, highlighting the environmental benefits and favorable thermal properties of the composite (Zakaria et al., 2022). Sentang is also widely used in Papua New Guinea as raw materials to make canoes (Lim et al., 2006).

In addition, the shoots of sentang are used as a vegetable as they are edible and eaten for traditional medicinal uses. As stated above, the tree contains azadirachtin ($C_{33}H_{44}O_{16}$), which can be used as an insect repellent and was reported effective in controlling over 195 insects, including armyworms and caterpillars. Additionally, azadirachtin compound can be used for medicinal purposes such as heart disease, psoriasis, nerve disorders, diabetes, eczema, and blood pressure (Isman et al., 1990; Zhong et al., 2017; Bernardes et al., 2018; Kurose et al., 2005; Kaewnang-O et al., 2011, Hummel et al., 2016; Rahmawathi et al., 2017). Moreover, the seed contains oil for soap production (Mak-Mensah & Firempong, 2011).

2.5 Macroscopic Characteristics of Wood

Many characteristics of wood can be easily observed with the naked eye, and these features are of significance because they provide insights into the growth conditions, reveal its physical properties, and assist in the process of wood identification (Ruffinatto et al., 2015; Ruffinatto & Crivellaro, 2019).

Figure 2.3 shows a cross-section of a hardwood stem. Although it is a tropical hardwood, the figure shows that the growth rings appear as distinct alternating bands of earlywood and latewood. It was reported that sentang tends to form diffuse-porous, with the pore diameter in the early growing season being the same size later in the year and has a slightly coarse and uneven texture (Gan et al., 1999; Iswanto et al., 2010).

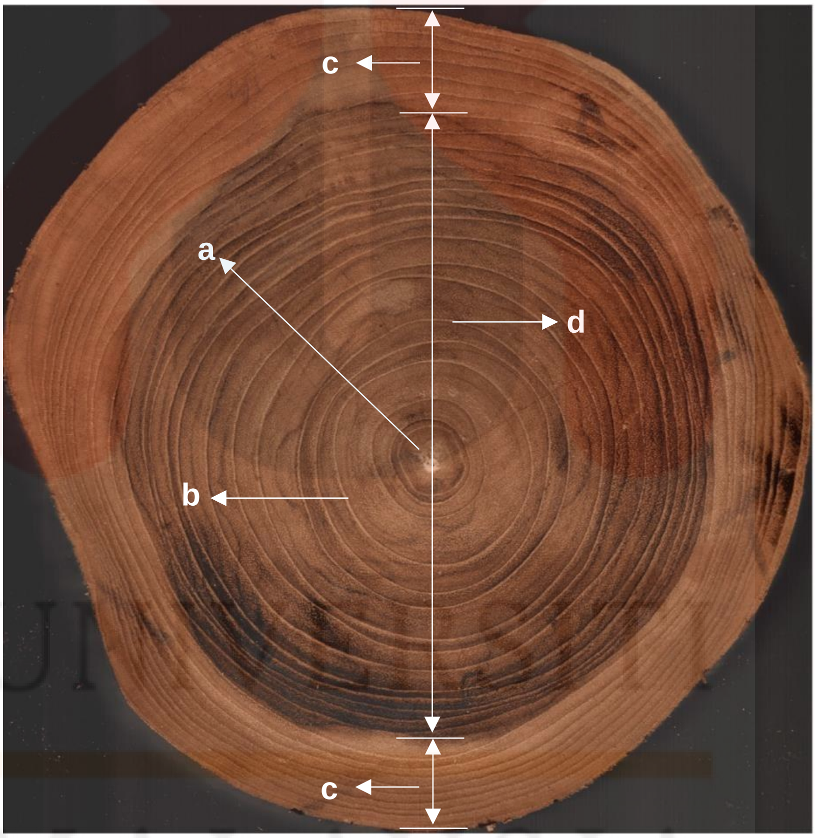

Source: Bahtiar et al. (2023) with modification

Figure 2.3: Cross-section of a hardwood stem showing the pith (a), annual growth ring (b), sapwood (c), and heartwood (d)

Examination of the cross-section image above reveals a dark-colored area surrounded by a lighter-colored area in the center. The dark area is called heartwood, while the lighter area is sapwood, where the cells are still alive. However, the inner portion of the sapwood, where most of the cells are no longer alive, still plays a role in conducting water upwards within a living tree. On the other hand, heartwood no longer possesses physiological functionality as the cells in this area are deceased, and thus, the primary function is for mechanical support (Shmulsky & Jones, 2019; Kang et al., 2021). It was reported that the sapwood of sentang has a straw-colored or pale red color and is moderately differentiated from the heartwood, which has a reddish-brown color (Gan et al., 1999; Hossain & Jalil, 2018).

2.6 Microscopic Structure of Hardwood

Hardwood is well known to be composed of widely varying proportions of different kinds of cells and thus often forms a unique and spectacular decorative appearance. Therefore, hardwood is widely used as raw material for furniture, paneling, and other decorative purposes. Table 2.3 describes that hardwoods consist of at least four significant types of cells, including fiber, vessel, longitudinal parenchyma, and ray parenchyma cells (Shmulsky & Jones, 2019).

Figure 2.4 shows the scanning electron microscopic (SEM) image of the cross-section of a hardwood. The figure presented various cells, such as fibers, vessels, and ray parenchymas. Fibers (fiber tracheids) are long, tapered, and usually thick-walled cells of hardwood xylem. The figure shows that the fibers tend to be rounded in cross-section. It is a well-established fact that the primary function of fibers in hardwood is to provide mechanical support. In addition, the density and strength of hardwoods are typically linked to the portion of the wood volume occupied by fibers relative to that of vessels, and the greater the proportion of thick-walled fibers, the higher the density and strength (Mendoza et al., 2019; Shmulsky & Jones, 2019). It was reported that 10-year-old sentang has an average fiber length of 890–1126 µm (Nordahlia et al., 2014).

Table 2.3: Major hardwood cell types.

Cell type	The proportion of xylem volume accounted for by cell type* (%)
Fiber tracheid†	15 – 60
Vessel element	20 – 60
Longitudinal parenchyma	0 – 24
Ray parenchyma	5 – 30

* The relative proportion of various cell types is relatively consistent within a species. The proportions of various cells can vary widely between species and species groups (genera).

† This category includes several cells: variations of true fiber tracheids and transition elements between fibers and vessel elements or between fibers and longitudinal parenchyma.

On the other hand, vessel elements typically have a much larger diameter than other longitudinal cells but are shorter in length than fibers. The short length of vessel elements is attributed to the fact that they often do not increase vertically during the maturation process and may even end up shorter than the cambial initials from which they originated (Olson et al., 2020). Typically, several vessel elements align end to end along the wood grain, creating extended tubular structures called vessels, which primarily serve for conducting water. It was reported that sentang has solitary vessels or multiples of up to 5 or rarely more, commonly clustering up to 4–5 vessels. The vessel tends to be arranged in tangential and radial series of up to 4 vessels with a round to oval shape, sometimes filled with the deposition of dried extractives, especially in heartwood (Nordahlia et al., 2013).

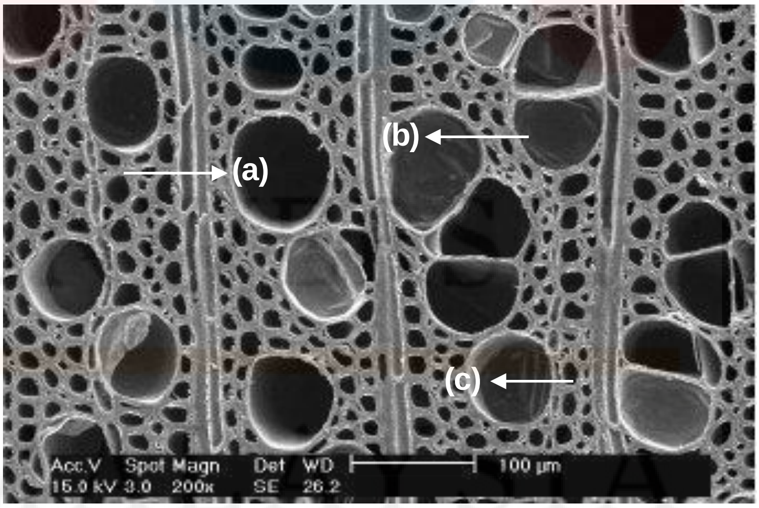

Source: Kang et al. (2011) with modification.

Figure 2.4: SEM image of a cross-section of a hardwood showing fiber (a), vessel (b), and ray parenchyma (c) cells

Furthermore, wood rays consist of parenchyma cell layers extending radially inward from the cambium. Ray parenchyma cells are typically divided into uniseriate rays, with only one cell in width when viewed in a tangential section. The others are multiseriate rays with two or more cells in width. Hardwood rays can vary in width tangentially from 1 to 30 or more cells. In contrast, softwood rays are generally one and, occasionally, two cells in width (Shmulsky & Jones, 2019). A brief observation from the figure, the ray parenchyma of sentang wood is uniseriate or biseriate. However, detailed observation is needed to confirm the type of ray parenchyma of the wood.

2.7 Physical Properties of Wood

2.7.1 Moisture Content (MC)

It is widely recognized that the MC of wood significantly impacts its properties, including density, strength, resistance to biological deterioration, and dimensional stability (Simpson & TenWolde, 1999). In green wood, moisture exists in free water in the cell lumens and bound water in the cell wall (Shmulsky & Jones, 2019). Thus, the MC of green wood is calculated as the combined weight of free and bound water, expressed as a percentage of the oven-dry (OD) weight of the wood. The MC of green wood differs from species to species and is often influenced by the wood density. As a general trend, when wood density increases, the volume of the cell lumens typically decreases. Consequently, the moisture content of green wood tends to decrease as wood density increases. (McDonald et al., 1995; Niklas & Spatz, 2010).

It is widely recognized that the cell wall is predominantly composed of cellulose and hemicellulose. Hydroxyl groups on these polymers render the cell wall highly hygroscopic, giving it a strong affinity for water (Song et al., 2014; Shmulsky & Jones, 2019). As moisture is lost in the green wood due to exposure to atmospheric conditions, a point where all the free water in the lumen has been removed but the cell wall is still saturated is termed the fiber saturation point (FSP) (Shmulsky & Jones, 2019). It was reported that the FSP ranges from 25% to 30% MC depending on the wood species, and the other study reported that FSP obtained through different methods may vary from 13% to 70% (Feist & Tarkow, 1967; Babiak & Kúdela, 1995). The FSP is critical because changes in MC below this point can significantly impact wood properties. For instance, dimensional shrinkage becomes remarkable, leading to distortion when the MC is lower than the FSP (Elustondo, 2010). Accordingly, the wood dimensions are almost unchanged unless the MC decreases to lower than the FSP in equilibrium with the surrounding climate. In addition, mechanical properties generally increase as the

MC decreases (Korkmaz & Büyüksarı, 2019).

As stated above, the green wood lost its moisture immediately after exposure to the atmospheric condition, and eventually, the MC of the wood reached a balance with the surrounding climate, called equilibrium moisture content (EMC) (Mitchell, 2018). Accordingly, the EMC of the wood is influenced by temperature and relative humidity, and several authors have well documented the EMC of wood at temperatures below 100℃ (Simpson, 1971).

2.7.2 Density

Density is defined by dividing the mass of wood by its volume at a specific MC. The density of wood is considered the most crucial physical property because it is closely correlated with many other mechanical and physical properties of the wood (Zhang, 1995). It is well known that the strength and stiffness of wood increase with density. In addition, the density influences the shrinking and swelling characteristics, although the relationship is not as direct as it is with strength properties (Saranpää, 2003).

Many factors affect the density, primarily attributed to the growth patterns of the tree, which alter the anatomy and chemical compound of the cells (Zhang, 1995). Generally, density strongly depends on the amount of cell wall material in the overall volume of the wood and increases as the proportion of cells with thick cell walls increases. However, in hardwoods, density is also influenced by the amount of void space occupied by vessel and parenchyma cells and the cell wall material (Dadzie & Amoah, 2015). Therefore, some tropical hardwoods have a density above 1,000 kg/m^3, while balsa has a density of roughly 60–380 kg/m^3 due to its larger vessel, an abundance of axial and ray parenchyma cells, and very thin-walled fiber (Azmi et al., 2022; Borrega & Gibson, 2015). On the other hand, sentang is categorized as light-hardwood with an air-dry density of 550–780 kg/m^3 (Nordahlia et al., 2013).

2.7.3 Swelling and Shrinkage

As stated above, when wood MC is lower than the FSP, it loses bound water, resulting in dimensional shrinkage. At this point, the removal of bound water molecules between the hemicellulose and cellulose molecules causes these chain molecules to move closer together, reducing the volume and subsequent shrinkage of the wood (Zitting et al., 2021). Thus, the shrinkage is proportional to the amount of bound water loss. Conversely, when moisture penetrates the cell wall of dry wood, the wood experiences swelling. This occurs as the moisture is absorbed by the cell wall components, causing the wood cells to expand and increase in volume.

It is well known that the shrinkage and swelling vary in the three distinct anisotropic directions of wood. Given that the S_2 layer of the cell wall is typically thicker than the other layers combined, the orientation of the microfibrils in this layer predominantly influences the extent of shrinkage. In the S_2 layer, most microfibrils align almost parallel to the longitudinal axis of the cell. Consequently, both transverse cell dimensions are affected, while the length of the cell remains relatively unaffected as the cell wall undergoes shrinking or swelling. Therefore, the most remarkable dimensional change occurs in the tangential direction, followed by the radial and longitudinal directions (Schulgasser & Witztum, 2015). Sometimes, shrinkage in the longitudinal direction is negligible for most practical purposes.

Generally, some factors, such as wood density, affect wood shrinkage (Jankowska et al., 2017). As stated above, shrinkage usually correlates to the water extracted from the cell wall. This implies that a species with higher density, possessing a thicker cell wall, would typically exhibit more significant shrinkage per unit of MC change than a species with lower density. However, the extractive compound that tends to reduce the FSP and bulk up the cell wall could affect the magnitude of the shrinkage, suggesting that heartwood tends to be more dimensionally stable than sapwood (Choong & Achmadi, 1991). On the other hand, sentang wood was reported to have low shrinkage, with an average shrinkage of 0.5 and 1.2% in radial and tangential directions, respectively (Wong et al., 2002).

2.8 Mechanical Properties of Wood

The mechanical properties of wood include its strength and ability to resist deformation. These properties involve various measurements, including resistance to deformations and distortions (elastic properties), properties related to failure under load (strength properties), and other factors related to wood performance (Winandy & Rowell, 2012). In this regard, mechanical properties are typically the most crucial characteristics of wood, especially in structural applications. Table 2.4 summarizes the essential mechanical properties of wood.

Table 2.4: Some essential mechanical properties of wood.

Properties	How or where is this property important
Strength properties	
Breaking strength (MOR)	Determines the maximum load a beam can withstand before rupture.
Compression strength parallel to the grain	Determines the maximum load a short post or column can support before collapses.
Compression perpendicular to the	It is essential in designing the connections

grain	between wood members in a building and the supports for a beam.
Tension strength parallel to the grain	It is necessary for the bottom member (chord) in a wood truss and for designing connections between wood members.
Shear strength parallel to the grain	It frequently plays a crucial role in establishing the load-carrying capacity of short beams.
Toughness	Measure the work required to fracture a small specimen in impact bending.
Resilience	It is measured by the amount of energy absorbed when the wood is deformed within its elastic range.
Side hardness	Determines the resistance to denting wood flooring.
Tension perpendicular to the grain	It is crucial in the design of the connections between wood members in a building.
Work to the maximum load	Measure the energy absorbed by a specimen as it is gradually bent to the point of reaching its maximum load.
Elastic properties	
Modulus of elasticity	Measure the resistance to bending related to the stiffness of a beam. Also, a factor in the strength of a long column to withstand buckling under compressive loads.
Modulus of elasticity parallel to the grain (Young's modulus)	Measure the resistance to elongation or shortening of a specimen under uniform tension or compression along the grain direction.

Source: Shmulsky & Jones (2019).

This study discussed some mechanical properties, such as the bending strength properties, including the modulus of rupture (MOR), modulus of elasticity (MOE), and compression strength of Sentang wood. As shown in the table, the MOR reflects the maximum load-carrying capacity of wood in bending. It is proportional to the maximum moment a wood specimen can withstand before ruptures and is generally an accepted measure of wood strength. On the other hand, the MOE reflects the deformations due to low stress that are ultimately recoverable after the stress is released. While compressive strength parallels to the grain represents the ability of wood to resist the compression forces applied in the direction of the wood grain (Green et al., 1999).

In general, the strength of wood is strongly correlated with density, and it is sufficient to predict an accurate estimation of wood strength based only on the density, regardless of the species (Zobel & Jett, 1995). As the density depends on the cell wall thickness, the mechanical properties of wood are also influenced by the anatomy of the cell wall. Sentang wood is reported to be moderately strong and classified as light-hardwood timber in Malaysia. The bending properties of sentang wood were 60 MPa and 6,770 MPa for MOR and MOE, respectively, while the compression strength was 31 MPa (Noraini, 1997). It is well known that light-hardwood timber is not naturally durable in tropical climates. However, it is relatively durable when exposed to temperate conditions, with a density below 720 kg/m^3 at 15% MC (Menon et al., 2004).

2.9 Variation in Wood Properties

Wood, being a natural product, exhibits inherent variability in its properties. The variability in wood properties occurs among species and genera, provenance, site location, and each tree itself. Therefore, although grown under the same site and age, the variability of tree-to-tree wood properties within species is so large that it could differ considerably among the species (Zobel & van Buijtenen, 1989).

It is widely recognized that most trees exhibit distinct patterns in wood properties within the annual growth ring, in the radial (from the pith to the bark) and longitudinal (from the base to the top) directions of the tree. The presence and proportion of earlywood and latewood within an annual growth ring due to environmental or genetic differences and their interactions are significant factors that influence the variability in wood properties within the tree (Diaz et al., 2018). For instance, the most significant variability in density occurs within the earlywood and latewood. This variability substantially impacts the overall wood density, particularly in the ring-porous hardwoods with large-sized vessel elements formed in the early growing season, followed by numerous smaller but thick-walled fibers (Zobel & van Buijtenen, 1989).

Wood properties can also vary significantly in the radial and longitudinal directions of the tree due to the age and location of the cambium relative to the pith. These variations are partly influenced by the properties of the juvenile wood and its distribution within a tree. The cambium, which is responsible for the secondary growth of the tree, generates different types of wood as the tree ages. Typically, juvenile wood is located near the pith, while mature wood is found further away from the pith. As the juvenile wood produces along the tree life, the topmost part of an old tree primarily consists of juvenile wood, which generally has similar characteristics to the wood formed in the earlier years at the lower part of the same tree (Zobel & Sprague, 1998).

In general, juvenile wood differs significantly from mature wood, showing distinct variations in wood properties along the radial and longitudinal direction of the tree. For instance, juvenile wood typically has a lower density, shorter and thinner-walled tracheids and fibers, and exhibits greater microfibril angles in the S_2 layer of cell wall than mature wood. In addition, MC varies greatly from juvenile to mature wood (Shmulsky & Jones, 2019). However, it was reported that juvenile wood has a slightly lower density or shorter fibers than mature wood in most hardwoods. Therefore, hardwood has more homogeneous wood properties along the radial and longitudinal directions of the tree than softwood (Jett & Zobel, 1975; Zerges & Newman, 1980).

2.9.1 Variation in the Radial Direction of the Tree

Wood properties vary among many species, and sometimes, there is a specific pattern in the radial direction of the tree, from the pith to the bark. As stated above, this pattern refers to features of juvenile wood located at the center of the stem surrounded by mature wood. Table 2.5 summarizes the radial variation patterns of some hardwood properties, showing all possible wood density patterns appearing in the hardwoods. The middle to high-density diffuse-porous hardwoods typically indicate a specific pattern of a lower density near the pith, followed by an increase and constant toward the bark. The low-density diffuse-porous hardwoods tend to have a slightly higher density near the pith, although some species experience less variation in density distribution from the pith toward the bark. The ring-porous hardwoods exhibit a higher density near the pith, followed by a decrease and then an increase to some extent toward the bark (Zobel & van Buijtenen, 1989).

On the other hand, most studies on the radial variation patterns in hardwoods focus on fiber length and reported that the fibers are shortest near the pith of the tree (Barnett & Bonham, 2004; Kim et al., 2009). Variations in the dimensions of ray cells, vessel elements, and other cell types have been observed along the radial direction of hardwoods. However, these variations are typically not as prominent as the variations in fiber length. Therefore, the variation along the radial direction in wood properties other than the density could be confusing because nearly every possible pattern could occur. However, variation in the fiber length was reported to have a consistent pattern, which typically tends to increase from pith toward bark (Zobel & van Buijtenen, 1989). Thus, it is crucial to determine the variation in the pattern of wood properties for each species on which the trees are grown.

Table 2.5: Radial variations in wood properties of some hardwood

Species	Variations
Swietenia macrophylla	Specific gravity increases toward the bark.
Tectona grandis	Fiber length increases toward the bark.
Gmelina arborea	Density increases gradually toward the bark.
Populus tremuloides	Specific gravity was higher near the pith, followed by a decrease, then increased toward the cambium.
Acer saccharum	Specific gravity was higher near the pith, followed by a decrease, then increased toward the cambium.
Acacia melanoxylon	The density increased from 10% to 50% radial position, followed by constant density up to 90% radial position from the pith.

Sources: Zobel & van Buijtenen (1989), Machado et al. (2014)

2.9.2 Variation in the Longitudinal Direction of the Tree

Similar to variation in the radial direction, many trees have a specific pattern in wood properties in the longitudinal direction of the tree. In species with a substantial distinction between juvenile and mature wood, variation in wood properties with height is automatic due to the increasing prevalence of juvenile wood from the bottom to the top of the tree (Zobel & van Buijtenen, 1989). Table 2.6 summarizes the variation patterns in the specific gravity of hardwood in the longitudinal direction of the tree.

Table 2.6: Longitudinal variations in specific gravity of some hardwood

Species	Variations
Swietenia macrophylla	Specific gravity was higher at the base, followed by a decrease and increased toward the crown.
Gmelina arborea	Specific gravity decreased from 0.41 to just 0.39 as tree height increased.
Populus tremuloides	Specific gravity was higher at the base, followed by a decrease and constant toward the crown.
Liriodendron tulipijera	Density was higher near the ground, gradually decreasing until it reached a plateau.
Nyssa sylvatica	There was essentially no difference in wood density along the longitudinal direction of the tree.
Acacia melanoxylon	The density experienced an increase with the height, more notably from 35% to 65% of the tree height.

Sources: Zobel & van Buijtenen (1989); Machado et al. (2014).

Some species showed a higher specific density at the bottom, then decreased and subsequently increased toward the merchantable top of the tree, while other species experienced a gradual increase toward the top of the tree. In addition, the longitudinal position event had no impact on specific gravity in the other tree, as indicated in Table 2.6. Although almost all conceivable patterns in wood properties along the longitudinal direction could appear in hardwoods, their magnitude is generally minor and thus does not significantly affect the utilization of the wood (Zobel & van Buijtenen, 1989).

2.10 The Effect of Growth Rate on Wood Properties

Many studies have been reported on the effect of radial growth rate on wood properties. Generally, growth ring width, structure, and uniformity affect the wood properties that define wood quality, and each can be influenced by alterations in radial growth rate. It was reported that a faster-growth tree tends to have a wider growth ring and a significant amount of juvenile wood. Thus, the wood would have characteristics unsuitable for high-quality timber products. The influence of growth rate extends to cell dimensions, specific gravity, and moisture content. Typically, faster-growing trees exhibit specific general patterns with shorter tracheids and fibers (Bannan, 1967). In addition, fast-growth ring-porous hardwood was reported to have more dense wood. However, an exception was reported in diffuse-porous hardwood, where variations in radial growth rates were found to have a minimal impact on wood properties (Khurshudyan, 1958; MacDonald & Franklin, 1969; Kazumi, 1983).

The relationships of the radial growth rate of some hardwoods to specific gravity are summarized in Table 2.7. The table shows no consistent relationship between specific gravity and radial growth rate was noted. A fast-growth ring-porous *Tectona grandis* exhibits a higher density, while the radial growth rate does not affect a diffuse porous *Gmelina arborea* density. Thus, any relationship between radial growth and wood properties seems not only to depend on the species but also on other factors.

Table 2.7: Relationship of radial growth rate to specific gravity in some hardwoods

Species	Comments
Tectona grandis	Fast-growing trees exhibited a slightly higher specific gravity.
Swietenia macrophylla	Specific gravity showed an increase with the radial growth rate.
Eucalyptus alba	The basic density does not exhibit any correlation with the radial growth rate.
Gmelina arborea	Fast growth does not alter the wood density, making it well-suited for the efficient production of uniform timber.
Terminalia ivorensis	No statistical significance was observed between the basic density and ring width.

Source: Zobel & van Buijtenen (1989)

CHAPTER 3

MATERIALS AND METHODS

3.1 Field Site

The site involved a 4.0 ha private plantation located at 5°44’48” N, 101°44’37” E in Jeli, Kelantan, Malaysia. A total of 4000 saplings from Perak, Malaysia, were used to establish a small-scale sentang plantation in 1995. Light silvicultural treatment, such as pruning after six months of planting, was conducted. However, the plantation has been unmanaged since 2004, and some trees have been harvested for domestic purposes. The sentang site used in this study is presented in Figure 3.1.

Figure 3.1: Sentang site in Jeli, Kelantan, Malaysia

3.2 Tree Inventory

A tree inventory was conducted using a 1.0 ha circular plot containing approximately 300 sentang trees. To reduce effort due to resource constraints, thirty trees were randomly selected from this population, and the circumference of the trees at breast height was measured using a tape measure. The diameter of the trees at breast height (DBH) was subsequently calculated. The trees were then categorized into slow-, average-, and fast-growth trees based on their average DBH (d_{av}) and standard deviation (SD). In this study, the DBH of a slow-growth tree (DBH_{sg}), an average-growth tree (DBH_{ag}), and a fast-growth tree (DBH_{fg}) was defined as follows:

$$DBH_{sg} < d_{av} - SD \qquad (1)$$

$$d_{av} - SD \leq DBH_{ag} \leq d_{av} + SD \qquad (2)$$

$$DBH_{fg} > d_{av} + SD \qquad (3)$$

The inventory results showed that the slow-growth tree has a DBH (DBH_{sg}) below 310 mm, the average-growth tree has a DBH (DBH_{ag}) from 310 to 470 mm, and the fast-growth tree has a DBH (DBH_{fg}) above 470 mm. Figure 3.2 illustrates the cross-section at the breast height of the slow-growth, average-growth, and fast-growth sentang trees used in this study.

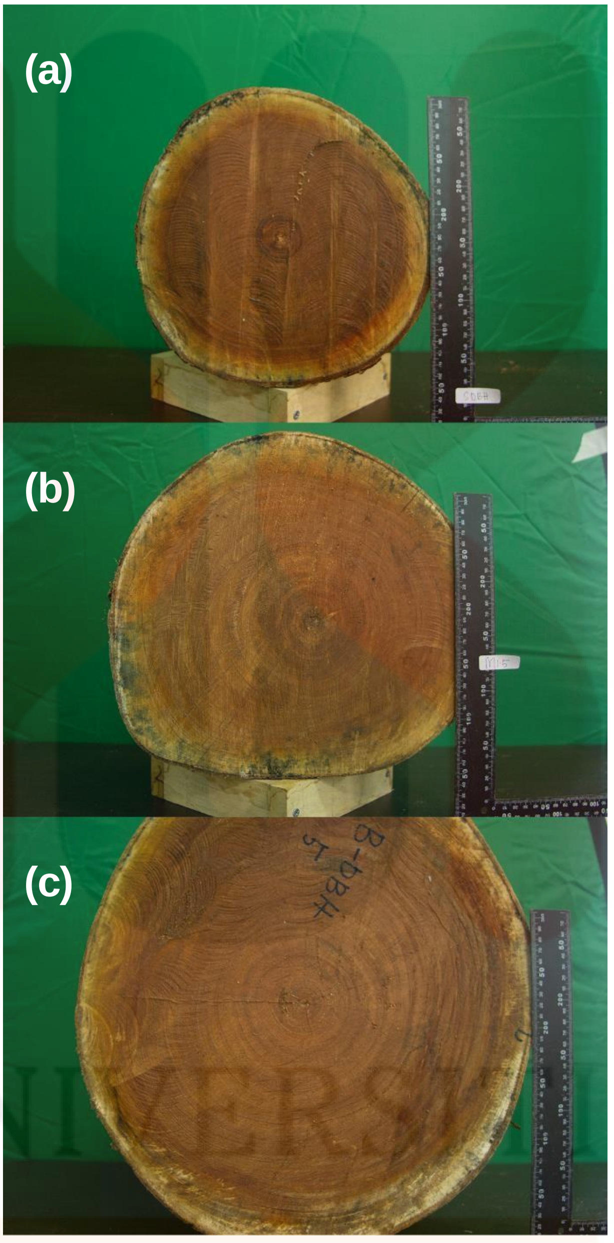

Figure 3.2: Cross section at the breast height of slow-growth (a), average-growth (b), and fast-growth (c) sentang trees

3.3 Sample Preparation

Three trees with the DBH of 300, 390, and 480 mm were selected for slow-, average- and fast-growth trees, respectively, and then harvested at 500 mm above the ground. After harvesting, the stems were cross-sectionally cut into 150 mm and 50 mm thick discs for the physical, mechanical, and anatomical properties evaluation at various heights, including at the bottom, the breast height, the middle (6 m above the ground), and the top (14 m above the ground) of the tree, as displayed in Fig. 3.3.

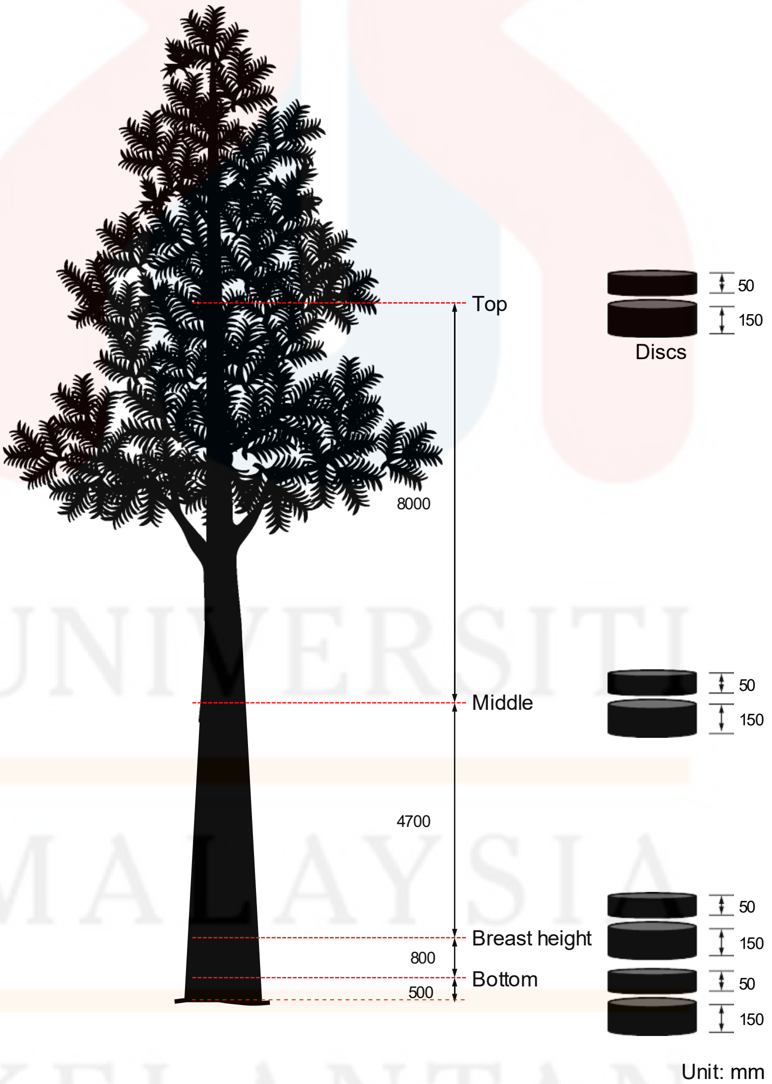

Figure 3.3: Discs collection from different tree heights for examination of wood properties in this study

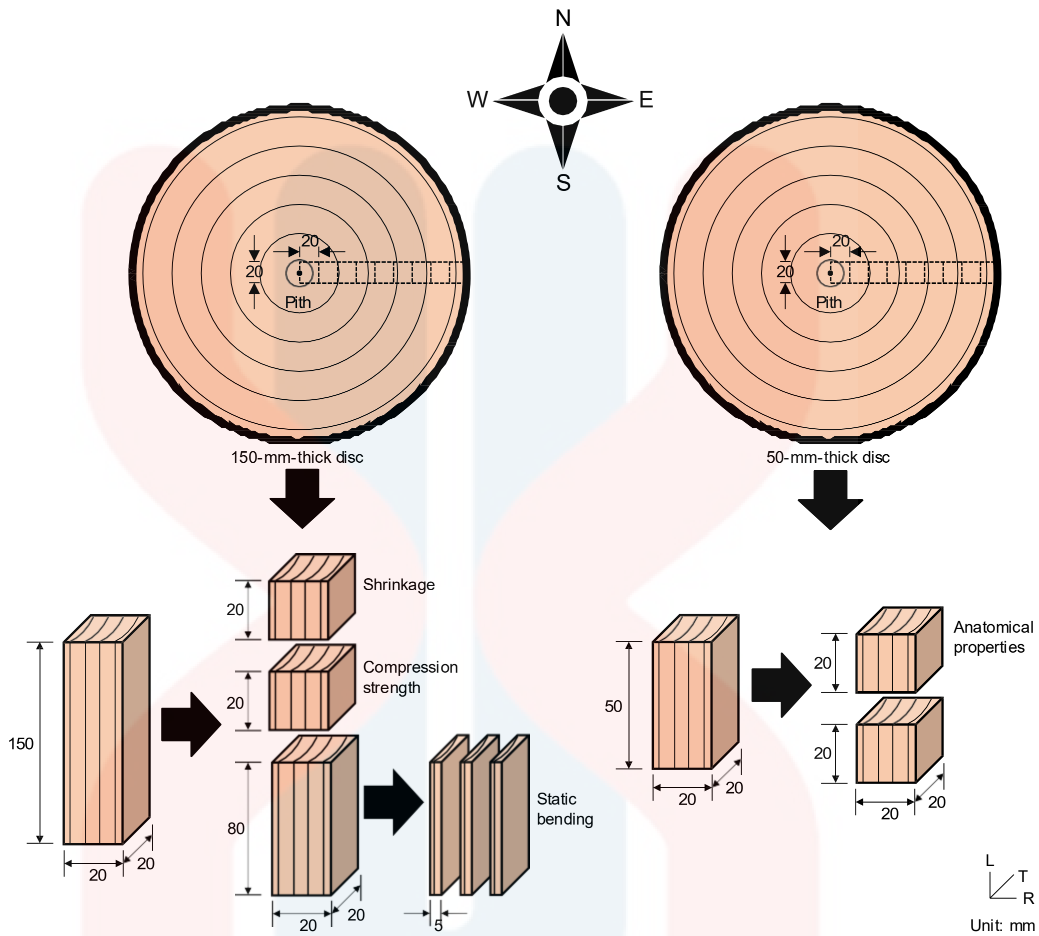

Figure 3.4: Cutting diagram of the sample used in this study

The east side of the 150-mm-thick discs was processed into consecutive sample sticks with a dimension of 20 (T) × 20 (R) × 150 (L) mm from the pith to the bark. The sample sticks were further processed into specific dimensions to evaluate the physical and mechanical properties of the wood along the radial direction. Same with the 150-mm-thick discs, the 50-mm-thick discs were processed into consecutive sample sticks with a dimension of 20 (T) × 20 (R) × 50 (L) mm from the pith to the bark. The sample sticks were then processed into sample cubes of 20 (T) × 20 (R) × 20 (L) mm for anatomical properties examination. The cutting diagram and dimensions of the samples for each test in this study are illustrated in Figure 3.4.

In addition, the research flow chart for this study is presented in Figure 3.5.

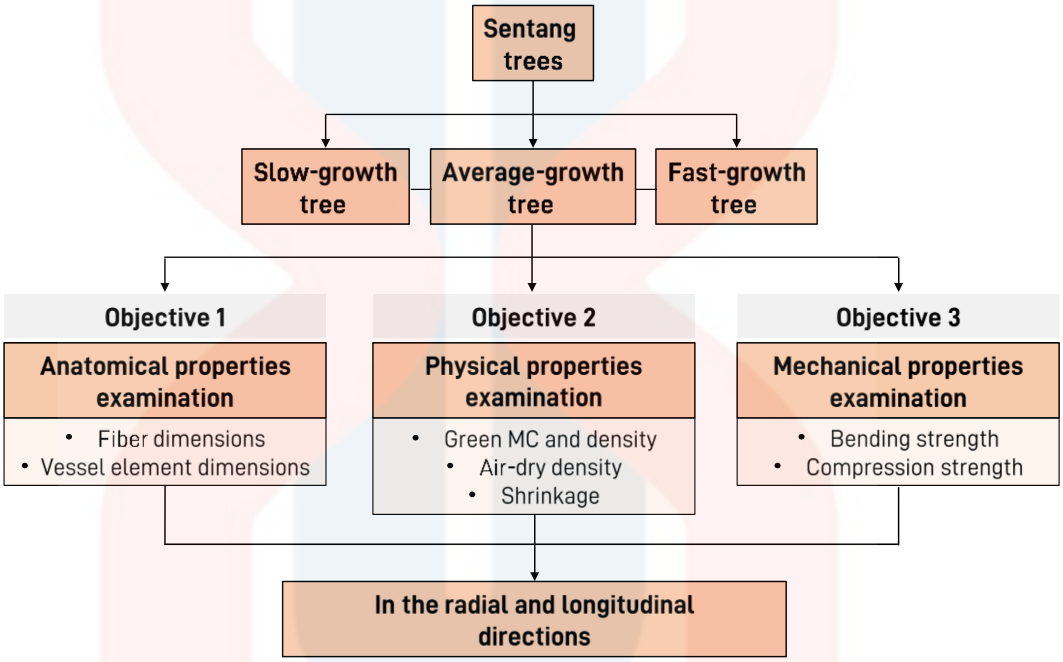

Figure 3.5: Research flow chart

3.4 Anatomical Properties Examination

The latewood of a cube sample obtained from each consecutive sample stick was then cut into match sizes and macerated according to the Schultze methods using 6 g of potassium chlorate and 100 mL of 35% nitric acid solution. Before microscopic observation, the macerated samples were crumbled and soaked in Safranin dye. The fibers and vessel elements were placed on a microscope slide with a calibration scale and randomly captured at 40 times magnification using a digital microscope (Leica DM750, Wetzlar, Germany). After calibrating the images using the scale in the microscope slide as a reference, a total of 50 latewood fiber lengths (L_f) and diameter (d_f) and 30 vessel element lengths (L_v) and diameter (d_v) were measured using the ImageJ software (NIH, 1.53k, Bethesda, MD, USA), as illustrated in Figure 3.6. The principle measurement technique using ImageJ is well described by Baviskar (2011).

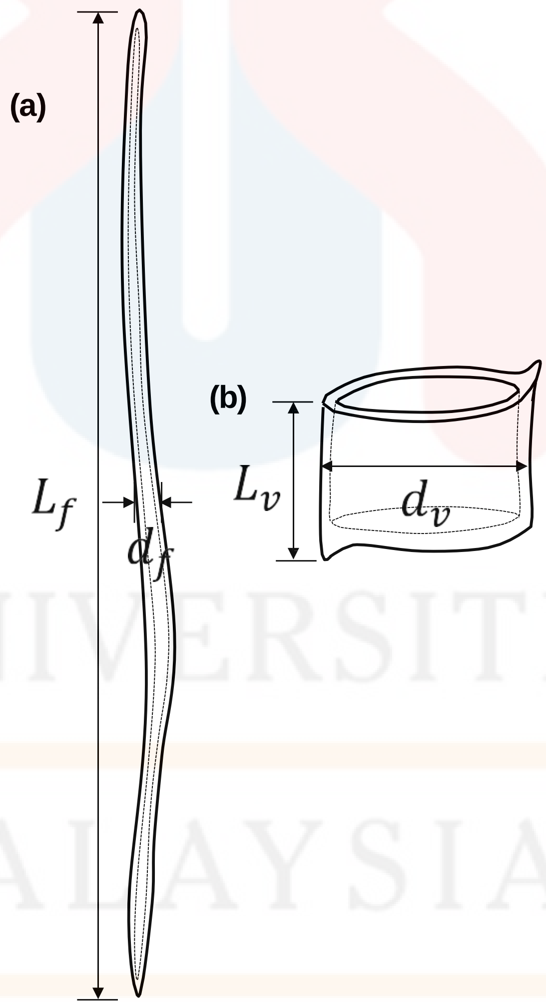

Figure 3.6: Fiber (a) and vessel (b) dimensions measurement

In addition, the scanning electron microscopy (SEM) image from the cross-section of slow-, average- and fast-growth trees was taken using SU3500, Hitachi High-Tech Corporation, Tokyo, Japan, for evaluating the anatomical properties, especially the vessel characteristics of all the categorized trees along the radial and longitudinal directions.

3.5 Physical Properties Examination

3.5.1 Shrinkage Measurement

The 20 (T) × 20 (R) × 150 (L) mm sample sticks were further processed into shrinkage samples with a dimension of 20 (T) × 20 (R) × 20 (L) mm, as illustrated in Figure 3.7. The samples were then air-dried, and the weight and dimensional changes in the tangential, radial, and longitudinal directions during the air drying were measured until a consistent weight was reached. Following the air-drying, the samples underwent an additional 24-hour drying period at a temperature of 40°C in the oven. The weight of the samples and dimensional changes in the tangential, radial, and longitudinal directions during the oven drying were also measured.

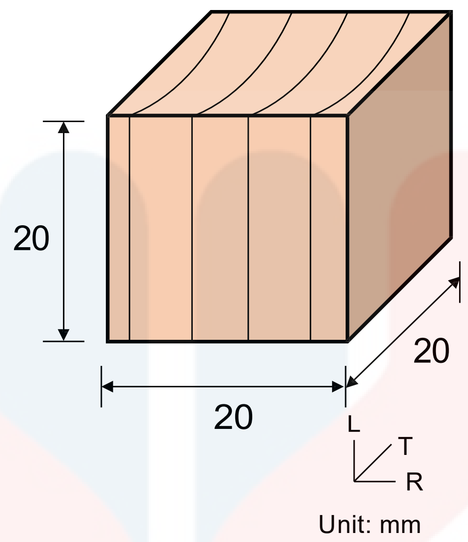

Figure 3.7: Sample for shrinkage measurement in the longitudinal, tangential, and radial directions

The calculation of shrinkage in the tangential, radial, and longitudinal directions was performed using the following equation:

$$\alpha_M = \frac{l_0 - l_M}{l_0} \times 100 \tag{4}$$

where α_M is shrinkage at M% MC, l_0 is a dimension at green MC, l_M is a dimension at M% MC. The shrinkage data in each direction were then plotted over its MC, and the shrinkage at an MC of 12% was then calculated using an exponential function based on the relationship between the shrinkage and its MC, as shown in Figure 3.8.

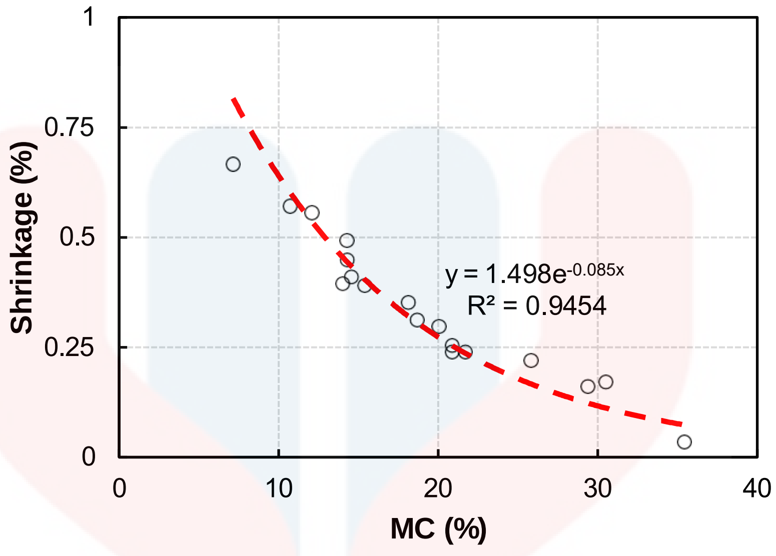

Figure 3.8: Relationship between the shrinkage in the longitudinal direction of the sample at 80 mm from the pith of the average-growth tree and its MC

3.5.2 Moisture Content (MC) and Density Measurement

After shrinkage measurement, air-dry density was calculated as the ratio of the mass of the sample before oven-drying at a temperature of 40°C to its volume. The samples were subsequently subjected to oven-drying at the temperature of 103°C for a duration of 24 h, and the MC was determined using the following equation:

$$MC = \frac{m_1 - m_0}{m_0} \times 100 \quad (5)$$

where m_1 and m_0 are green mass and mass of the samples after oven-dry, respectively. In addition, green density was defined as the ratio of the green mass of the sample to its volume.

3.6 Mechanical Properties Examination

3.6.1 Bending Strength Test

For a static bending test, the 20 (T) × 20 (R) × 150 (L) mm sample sticks were processed into a dimension of 20 (T) × 20 (R) × 80 (L) mm. The 20 (T) × 20 (R) × 80 (L) mm samples were further processed into three static bending samples with a dimension of 20 (T) × 5 (R) × 80 (L) mm. The test was conducted under the Japanese Industrial Standard (JIS Z2101, 2009) with slight modifications in the dimensions of the samples. Using a Universal Testing Machine (UTM), a load was applied at a 1 mm/min loading speed with a 70 mm span, as illustrated in Figure 3.9. The MOR and MOE of the sample were calculated using the following equations.

$$MOR = \frac{3PL}{2bh^2} \tag{6}$$

$$MOE = \frac{P_1L^3}{4d_1bh^2} \tag{7}$$

where MOR is the Modulus of Rupture (N/mm^2), MOE is the Modulus of Elasticity (N/mm^2), P is the maximum load (N), P_1 represents the load at the limit of proportionality (N), L is the span length (mm), b is the sample width (mm), h is the sample thickness (mm), and d_1 represents the deflection at the limit of proportionality (mm).

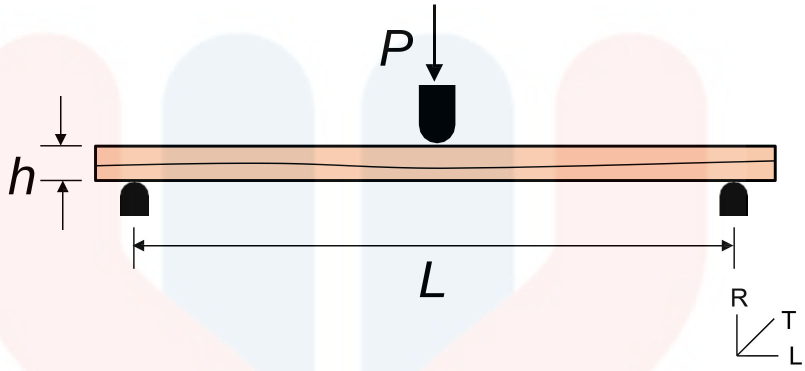

Figure 3.9: Schematic diagram of static bending test

3.6.2 Compression Strength Test

The 20 (T) × 20 (R) × 150 (L) mm sample sticks were further processed into compression strength samples with a dimension of 20 (T) × 20 (R) × 20 (L) mm. The test was conducted under the Japanese Industrial Standard (JIS Z2101, 2009) with slight modification in the specimen dimension in the longitudinal direction. Using the UTM, a load was applied parallel to the fiber orientation of the sample at a transverse section of the sample surface, as shown in Figure 3.10, with a 1 mm/min loading speed. The maximum load was recorded, and the compression strength parallel to the grain of the sample was calculated using the following equation.

$$F = \frac{P}{A} \quad (8)$$

where F is compression strength (N/mm^2), P is the maximum load (N), and A is the cross-section area of the sample (mm^2).

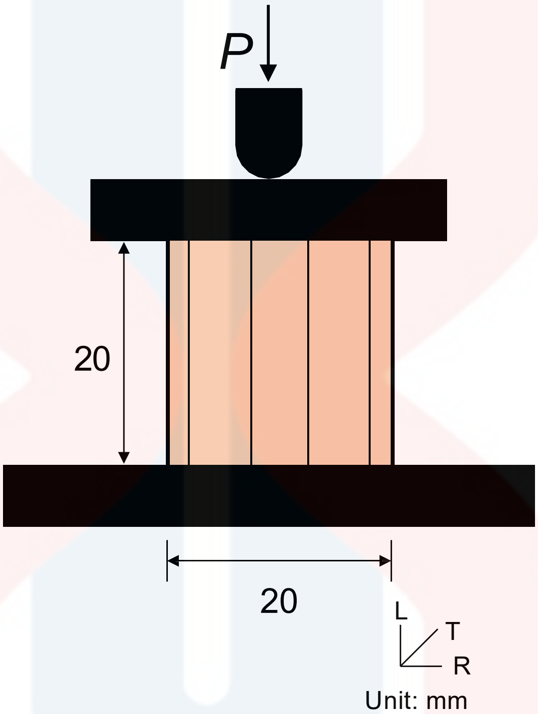

Figure 3.10: Schematic diagram of compression strength test

CHAPTER 4

RESULTS AND DISCUSSION

4.1 Anatomical Properties

4.1.1 Fiber Dimensions

Figure 4.1 presents the fiber length variations in the radial and longitudinal directions of all the categorized trees. The figure showed that the radial variation in the fiber length has varied patterns depending on the radial growth rate and longitudinal position. However, in general, the results can be summarized as follows: Except at the top of the tree, the fiber length of the slow-growth tree tends to decrease slightly after a few distances from the pith, followed by an increase toward the bark. A similar tendency was also observed at the breast height of the average- and fast-growth trees. A relatively constant fiber length was found in the middle of the average- and fast-growth trees. In addition, the fiber length at the top of all the categorized trees tends to increase gradually, while the fiber length at the bottom of the average- and fast-growth trees experiences a decrease from the pith to the bark.

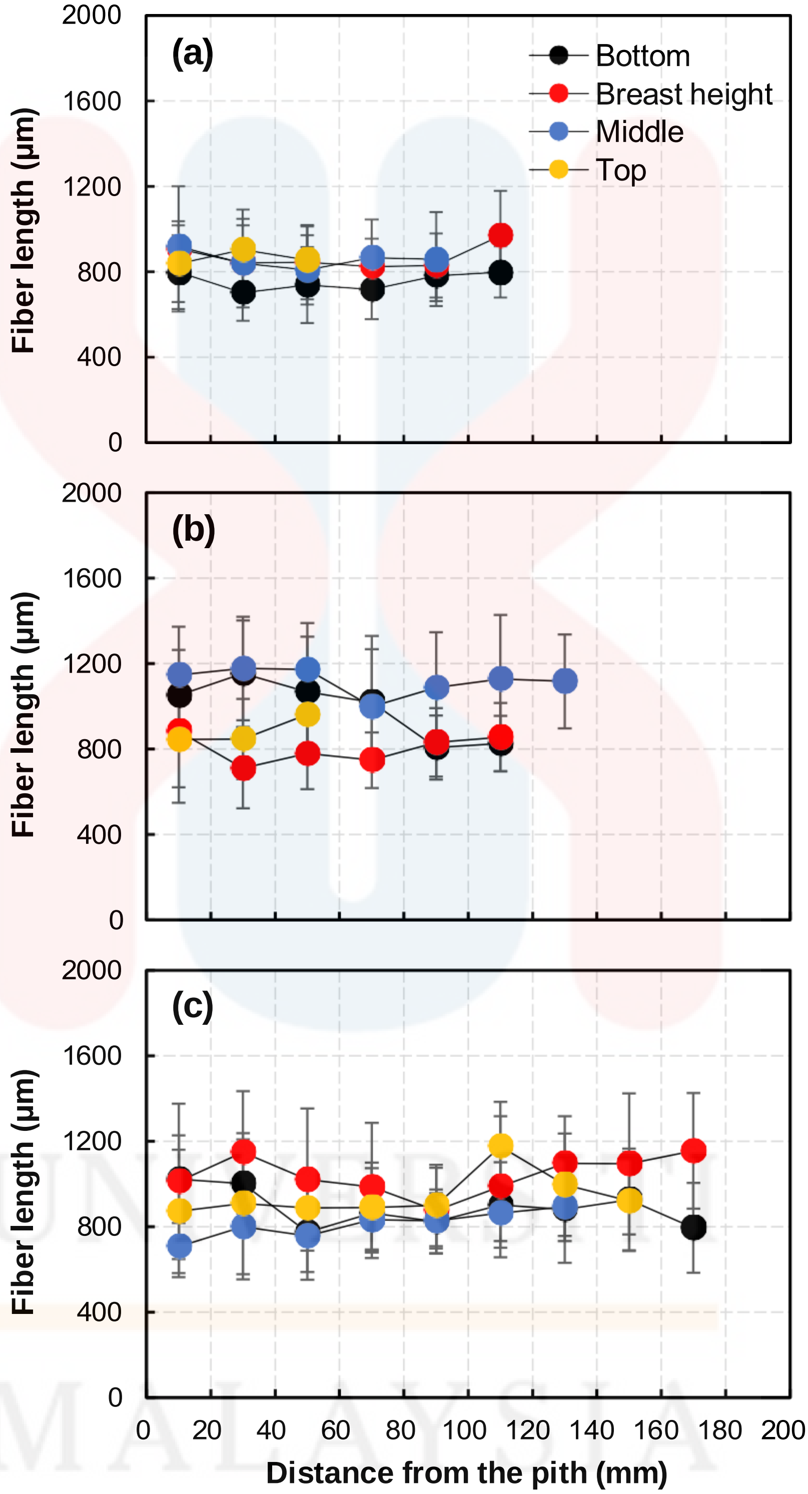

Figure 4.1: Fiber length variations in the radial and longitudinal directions of the slow- (a), average- (b), and fast-growth (c) trees

From the results above, the radial variation in the fiber length of the tree seems to have no persistent pattern, yet the tendency could be divided into four patterns, as shown in Table 4.1. The results seem different from the previous studies, mentioning that the fiber length near the pith generally has a shorter length due to the presence of juvenile wood (Evans et al., 2000). The other findings also mentioned that the fiber length of some fast-growing species planted in Malaysia and Indonesia increased toward the bark (Honjo et al., 2005; Wahyudi et al., 2016), leaving the underlying reason for these radial patterns found in this study remains unclear.

Table 4.1: Radial variations in the fiber length of all the categorized trees.

Categorized tree	Longitudinal position	Radial variation
Slow-growth	Bottom	Tend to decrease, followed by a constant increase toward the bark.
	Breast height	Tend to decrease, followed by a constant increase toward the bark.
	Middle	Tend to decrease, followed by a constant increase toward the bark.
	Top	Tend to increase toward the bark.
Average-growth	Bottom	Tend to decrease toward the bark.
	Breast height	Tend to decrease, followed by a constant increase toward the bark.
	Middle	Tend to have a constant fiber length from the pith to the bark.
	Top	Tend to increase toward the bark.
Fast-growth	Bottom	Tend to decrease toward the bark.
	Breast height	Tend to decrease, followed by a constant increase toward the bark.
	Middle	Tend to have a constant fiber length from the pith to the bark.
	Top	Tend to increase toward the bark.

Similar to the radial variation, the longitudinal variation in the fiber length also has varied patterns depending on the radial growth rate and radial position.

However, in general, the figure showed that the fiber length of the slow-growth tree tends to increase toward the top of the tree. In comparison, the fiber length of the average- and fast-growth trees tends to fluctuate. The fiber length of the average-growth tree experiences a decrease from the bottom to the breast height, followed by an increase to the middle and a decrease toward the top of the tree. While the fiber length of the fast-growth tree tends to increase from the bottom to the breast height, followed by a decrease to the middle, and then exhibits an increase toward the top of the tree.

In this study, the average fiber length was 833, 964, and 927 μm for slow-, average-, and fast-growth trees, respectively, suggesting that the slow-growth tree has a shorter fiber length than the other categorized trees. The results were similar to the fiber length of a 10-year-old sentang, which reported the average fiber length was 890–1126 μm (Nordahlia et al., 2014).

Figure 4.2 shows the fiber diameter variations in the radial and longitudinal directions of the trees. Despite the radial growth rate and longitudinal position, the radial variation in the fiber diameter has a typical pattern, exhibiting a relatively constant size from the pith to the bark, except at the bottom of all the categorized trees, showing a decrease toward the bark.

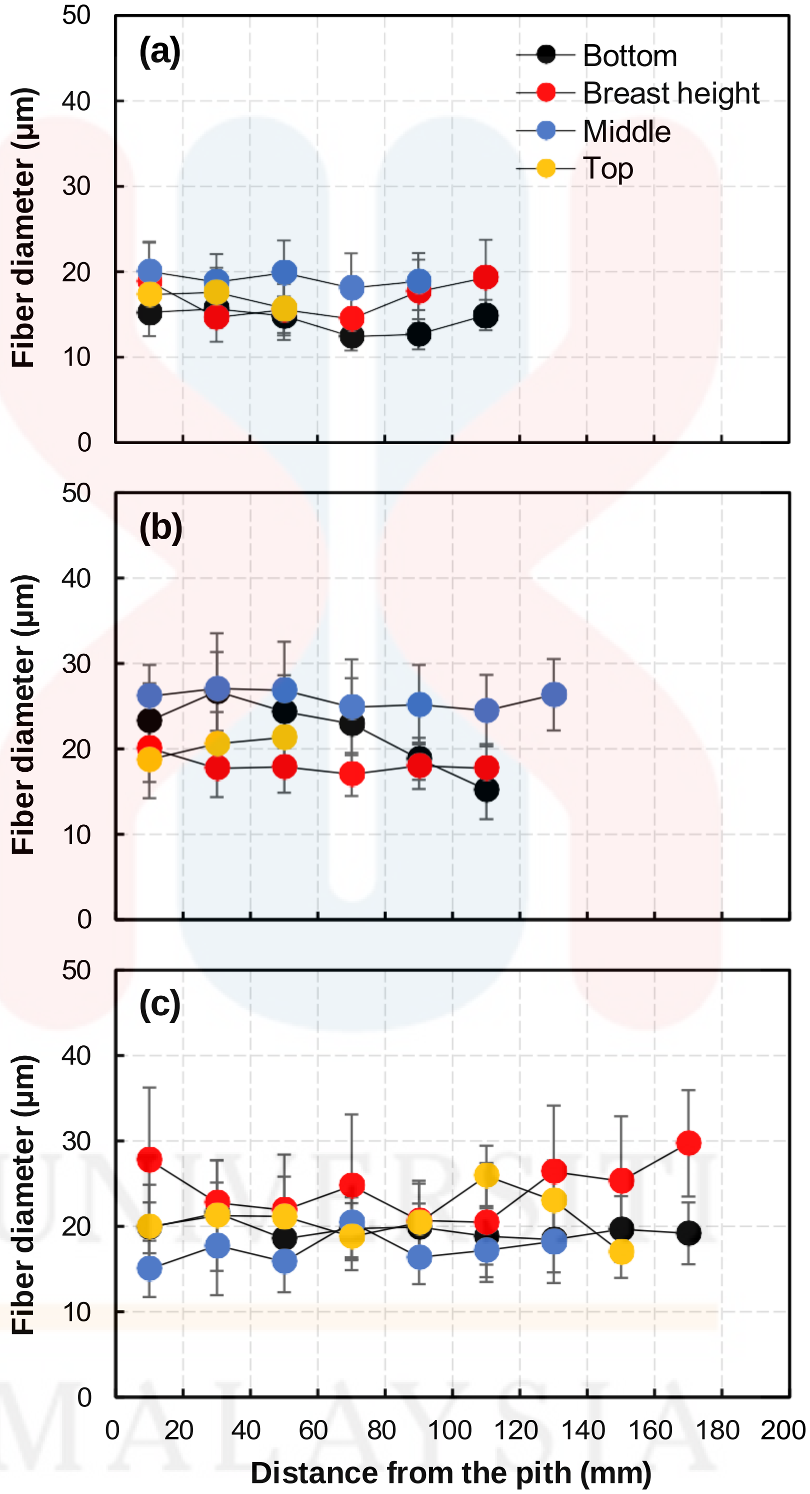

Figure 4.2: Fiber diameter variations in the radial and longitudinal directions of the slow- (a), average- (b), and fast-growth (c) trees

However, the figure showed that the longitudinal variations of the fiber diameter have varied patterns and fluctuate depending on the radial growth rate and radial position. In general, the figure demonstrates that the slow-growth tree exhibits an increase from the bottom to the middle, followed by a decrease toward the top of the tree. The fiber diameter of the average-growth tree decreased from the bottom to the breast height, followed by an increase to the middle and a decrease toward the bark. In contrast, the fast-growth tree experiences an increase from the bottom to the breast height, followed by a decrease to the middle and a slight increase toward the top of the tree.

In this study, the average fiber diameter was 16.6, 21.9, and 20.7 µm for slow-, average, and fast-growth trees, respectively, showing that the slow-growth tree tends to have a smaller fiber diameter than the other categorized trees.

It was documented that fiber dimensions play a crucial role in influencing the quality of pulp and paper products (Larsson et al., 2018; Przybysz et al., 2018), as well as wood products and wood composites (Wan et al., 2018). The above results confirmed that the fiber of the slow-growth tree tends to have a shorter length and smaller diameter than the other categorized trees, indicating that the fiber is more rigid and could have a higher wood density and mechanical properties. The fiber can potentially be less favorable as a raw material for paper manufacturing (Zhao et al., 2018).

4.1.2 Vessel Element Dimensions

Figure 4.3 presents the vessel element length variations in the radial and longitudinal directions of all the categorized trees. Despite the longitudinal position, the figure explained that the radial variation in the vessel element length of all the categorized trees has a typical pattern, showing a gradual increase toward the bark. A similar tendency was found in the other hardwood, which reported that the vessel length increased along the radial direction (Naji et al., 2013; Wang et al., 2021).

However, the longitudinal variation of the vessel element length has varied patterns and fluctuates depending on the radial growth rate and radial position. The figure shows that the vessel element length of the slow-growth tree tends to decrease from the bottom to the breast height, followed by a slight increase toward the top of the tree. The average-growth tree exhibits a relatively small increase from the bottom to the top of the tree. In contrast, the fast-growth tree experiences a decrease from the bottom to the middle, followed by an increase toward the top of the tree.

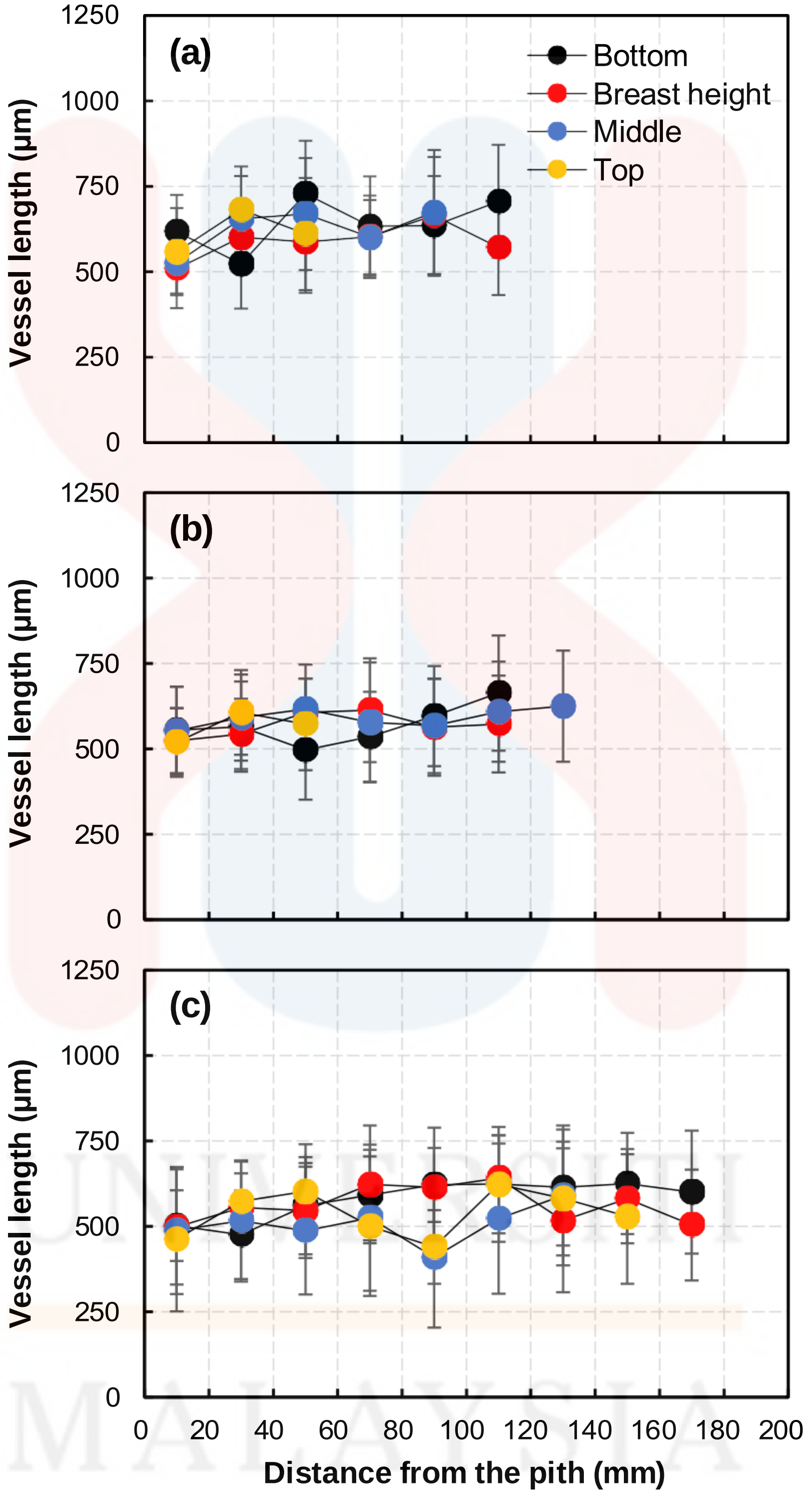

Figure 4.3: Vessel element length variations in the radial and longitudinal directions of the slow- (a), average- (b), and fast-growth (c) trees

In this study, the average vessel element length was 618, 576, and 550 µm for the slow-, average-, and fast-growth trees, respectively, suggesting that the slow-growth tree has a longer vessel element length.

Figure 4.4 shows the vessel element diameter variations in the radial and longitudinal directions of all the categorized trees. Similar to the vessel element length, the radial variation in vessel element diameter of all the categorized trees has a typical pattern of a gradual increase toward the bark. This tendency was confirmed by the SEM image shown in Figure 4.5, indicating a larger vessel element diameter at a sample cross-section near the bark than near the pith, and similar SEM images were observed in the other categorized trees. A similar finding was also reported in the vessel element of *Gmelina arborea*, where a rapid increase in diameter was observed until a certain distance from the pith, followed by a constant diameter size toward the bark (Hidayati et al., 2017).

However, the figure illustrates that the longitudinal variation of the vessel element diameter has varied patterns depending on the radial growth rate. The vessel element diameter of the average-growth tree tends to increase toward the top of the tree, while the other categorized trees have fluctuating patterns depending on the radial position.

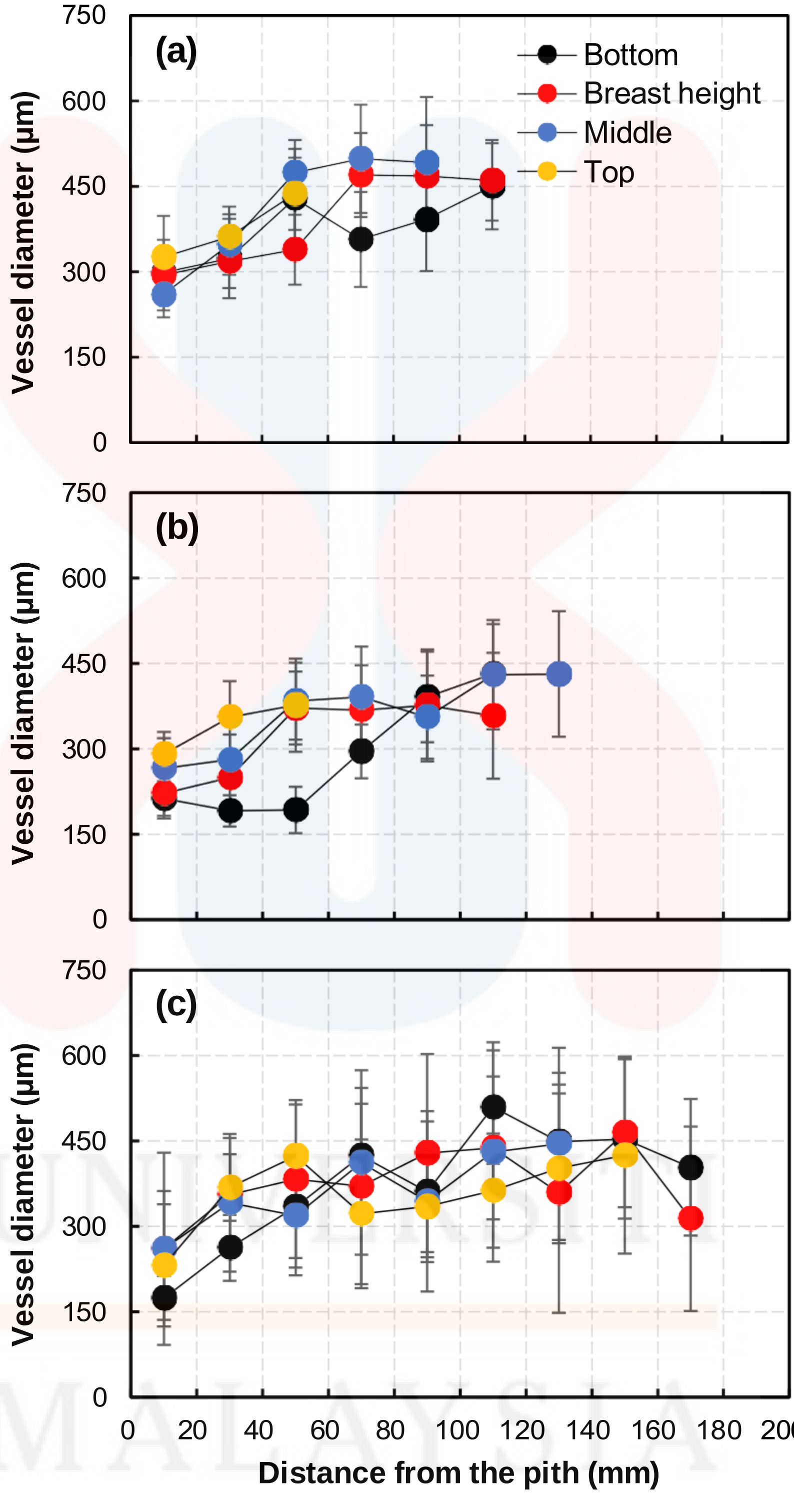

Figure 4.4: Vessel element diameter variations in the radial and longitudinal directions of the slow- (a), average- (b), and fast-growth (c) trees

In this study, the average vessel element diameter was 390, 328, and 369 µm for slow-, average-, and fast-growth trees, respectively, suggesting that the slow-growth tree has a larger vessel element diameter than the other categorized trees. The results seem much higher than the average vessel element diameter of a 10-year-old sentang of 137–155 µm (Nordahlia et al., 2014).

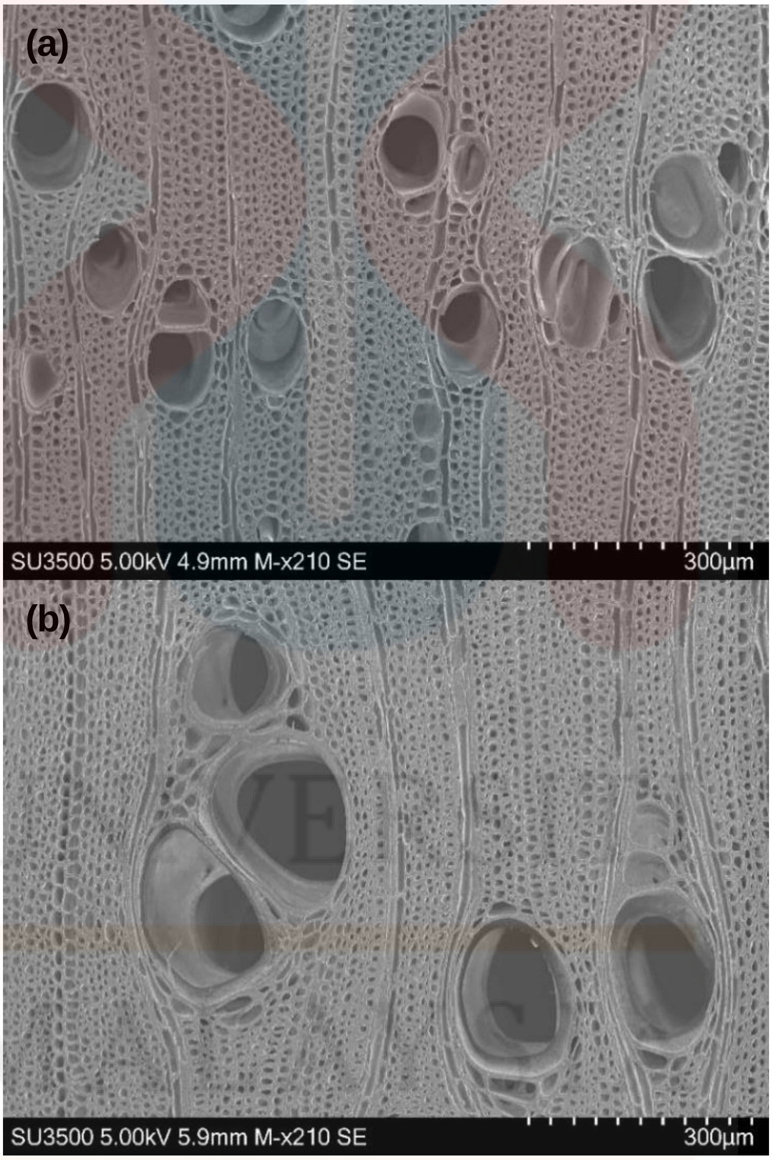

Figure 4.5: SEM image of a sample cross-section near the pith (a) and bark (b) of the slow-growth tree

From the results above, the slow-growth tree tends to have longer and larger vessel elements than the other categorized trees, likely attributed to a reduced rate of cell division in the cambium. It has been suggested that during periods of rapid growth, the cambial initials divide before attaining their maximum potential length (Zobel & van Buijtenen, 1989). As the primary function of the vessel is for liquid conduction, a longer and larger vessel positively affects the capacity of the tree to transport liquid.

4.2 Physical Properties

4.2.1 Green MC

Table 4.1 presents the green wood MC, green wood density, and air-dry wood density variations in the radial and longitudinal directions of all the categorized trees. The results showed that the radial variation in the green wood MC of all the categorized trees has a typical pattern, showing a gradual decrease toward the bark, except for the fast-growth tree. Several authors also reported a similar result, mentioning that the green wood MC was higher near the pith than the bark. This tendency is typical for some fast-growing species, including *Cedrela odorata*, *Acacia mangium*, and *Gmelina arborea* (Ofori & Brentuo, 2005;

Muñoz & Moya, 2008). A higher MC near the pith is probably due to the presence of juvenile wood. Some authors reported that juvenile wood has higher MC than mature wood (Zobel & Sprague, 1998; Tomczak et al., 2021).

On the other hand, the opposite tendency in the fast-growth tree could be attributed to the presence of heartwood and sapwood. It is generally known that the process of heartwood formation from sapwood occurs faster in the fast-growth tree, and heartwood often has a lower MC than sapwood. In this regard, it is understandable that the green wood MC of the fast-growth tree tends to increase toward the bark due to a more substantial amount of heartwood.

Similarly, the longitudinal variation of the green wood MC of all the categorized trees has a typical pattern, showing a decrease toward the top of the tree. The green wood MC often depends on the wood density, and generally, the MC decreases with increasing wood density (McDonald et al., 1995; Niklas & Spatz, 2010). Although the top of the tree typically contains more juvenile wood and, as stated above, the wood often has a lower density and thus has a higher MC than mature wood. However, the results suggested that the bottom logs of all the categorized trees contain more water than the top logs in green conditions, leaving the reason for this result remains unclear and needs further study.

In this study, the average green wood MC of slow-, average-, and fast-growth trees was 42.0, 39.3, and 48.4%, showing that the fast-growth tree tends to have a higher green wood MC. The results indicated that the timber obtained from the core of a bottom log of the fast-growth tree contains a considerable amount of water and juvenile wood. Thus, it is challenging to do further processes, such as drying, because juvenile wood with a higher MC could cause a significant drying defect.

4.2.2 Density

The table illustrates that the radial variation in the green wood density of all the categorized trees has a typical pattern, exhibiting an increase toward the bark. A similar tendency was also reported in the other fast-growing species, such as *Casuarina odorata* and *C. equisetifolia* (Ofori & Brentuo, 2005; Chowdhury et al., 2009). Various factors may affect green wood density, such as the presence of juvenile wood, cell types, and their size and proportion in the wood sample. It is well known that fiber and vessel element dimensions are some of the main factors affecting the density of hardwood. However, the dimension of these cells seems unrelated to the results, and thus, the presence of juvenile wood near the pith appears responsible for this finding, as juvenile wood typically has a lower density than mature wood. The other possibility is the proportion of the vessel element in the wood sample, suggesting that the vessel element was more concentrated at the sample near the pith than the bark. However, the vessel element distribution was not examined in this study, and thus, further investigation is suggested to confirm the vessel element distribution along the radial direction.

In addition, the results indicated that the longitudinal variation of the green density has varied patterns depending on the radial growth rate and radial position. The table showed that the green density of the slow-growth tree tends to decrease from the bottom to the middle, followed by an increase toward the top of the tree. A relatively similar tendency was also observed in the average-growth tree. In contrast, the green density of the fast-growth tree tends to increase toward the top of the tree. Although the top of the tree typically contains more juvenile wood, which often has a lower density than mature wood, the results revealed that the top of all the categorized trees tends to have a higher density, leaving the underlying reason for these results remains unclear.

In this study, the average green wood density of slow-, average-, and fast-growth trees was 689, 699, and 679 kg/m^3, indicating that the fast-growth tree has a lower green wood density than the other categorized trees.

Table 4.2: Green wood MC, green wood density, and air-dry wood density variations in the radial and longitudinal directions of all the categorized trees.

Tree categorize	Longitudinal Position	Distance from the pith (mm)	Green MC (%)	Green density (kg/m^3)	Air-dry density (kg/m^3)
Slow-growth tree	Bottom	0–20	41.2	669	573 (41)
		20–40	45.6	673	554 (14)
		40–60	45.9	688	567 (27)
		60–80	44.4	694	583 (38)
		80–100	37.4	667	574 (24)
		100–120	39.0	760	637 (23)
		120–140	35.5	723	615 (14)
	Breast height	0–20	-	-	509 (47)
		20–40	47.5	654	531 (16)
		40–60	42.8	680	570 (33)
		60–80	43.0	665	570 (20)
		80–100	43.8	703	590 (22)
		100–120	36.7	704	608 (12)
	Middle	0–20	-	-	424 (80)
		20–40	38.8	616	541 (11)
		40–60	45.1	681	566 (17)
		60–80	44.2	682	560 (18)
		80–100	44.7	692	590 (47)
		100–120	42.6	685	567 (26)
	Top	0–20	-	-	493 (113)
		20–40	42.1	755	615 (3)
		40–60	42.0	706	596 (18)
		60–80	38.5	691	609 (37)
Average-growth tree	Bottom	0–20	-	-	573 (22)
		20–40	49.2	729	607 (41)
		40–60	44.2	683	563 (17)
		60–80	47.3	750	616 (35)
		80–100	-	-	586 (12)
		100–120	44.6	728	605 (17)

		120–140	37.4	701	606 (19)
	Breast height	0–20	-	-	528 (77)
		20–40	46.4	673	556 (23)
		40–60	45.7	670	544 (13)
		60–80	43.9	706	593 (12)
		80–100	40.6	708	589 (13)
		100–120	35.3	653	584 (31)
		120–140	34.9	664	584 (14)
	Middle	0–20	-	-	468 (76)
		20–40	41.5	660	568 (15)
		40–60	39.2	730	610 (16)
		60–80	35.0	668	580 (3)
		80–100	39.3	699	588 (12)
		100–120	28.3	703	609 (5)
		120–140	39.4	696	591 (18)
		140–160	34.7	669	578 (20)
	Top	0–20	-	-	601 (77)
		20–40	31.0	743	664 (21)
		40–60	31.9	759	648 (12)
		60–80	34.5	706	647 (13)
Fast-growth tree	Bottom	0-20	-	-	520 (37)
		20–40	43.5	599	500 (6)
		40–60	46.3	626	511 (32)
		60–80	47.3	658	532 (39)
		80–100	42.9	594	476 (20)
		100–120	-	-	527 (34)
		120–140	-	-	540 (27)
		140–160	43.8	730	588 (13)
		160–180	47.8	669	557 (4)
		180–200	49.8	645	564 (15)
	Breast height	0–20	-	-	500 (14)
		20–40	-	-	474 (17)
		40–60	45.8	617	527 (5)
		60–80	45.2	631	523 (21)

	80–100	48.9	634	499 (35)
	100–120	49.3	616	503 (35)
	120–140	-	-	607 (76)
	140–160	55.8	724	560 (40)
	160–180	58.8	696	541 (24)
	180–200	49.2	687	574 (63)
Middle	0–20	-	-	445 (20)
	20–40	-	-	529 (30)
	40–60	43.7	648	537 (13)
	60–80	50.1	659	538 (16)
	80–100	43.4	623	579 (44)
	100–120	63.5	690	570 (42)
	120–140	49.7	731	579 87)
	140–160	65.2	714	579 (30)
	160–180	51.5	751	569 (33)
Top	0–20	-	-	559
	20–40	-	-	619 (12)
	40–60	40.1	720	655 (51)
	60–80	42.5	716	582 (13)
	80–100	43.4	749	641 (27)
	100–120	46.1	795	641 (39)
	120–140	43.0	734	585 (30)

Note: - is the measurement was not conducted.

On the other hand, the radial variation of the air-dry wood density has a similar tendency to the green wood density. The table generally describes that the air-dry wood density of all the categorized trees tends to increase gradually toward the bark. This tendency was mainly observed at the breast height and the middle of the trees. While at the bottom and top of the trees, the air-dry wood density tends to decrease after a few distances from the pith and then increases toward the bark.

The table shows that the longitudinal variation of the air-dry density has a tendency similar to that of the green density. The air-dry density of the slow-growth tree tends to decrease from the bottom to the middle, followed by an increase toward the top of the tree. A relatively similar tendency was also observed in the average-growth tree. In contrast, the air-dry density of the fast-growth tree tends to increase from the bottom to the top of the tree.

In this study, the average air-dry wood density of slow-, average- and fast-growth trees was 567, 587, and 550 kg/m^3, respectively, identifying that the fast-growth tree tends to have a lower air-dry wood density. This is probably due to a more significant amount of juvenile wood in the fast-growth tree. It has been reported that a faster-growing tree exhibits wider growth rings and lower wood density, primarily due to the significant presence of juvenile wood (Carino & Biblis, 2009; Karlsson et al., 2013; Carrasco et al., 2014).

4.2.2 Shrinkage

Table 4.2 presents the shrinkage variations in the tangential, radial, and longitudinal directions of all the categorized trees at an MC of 12%. The table shows that the radial variation in the shrinkage has varied patterns depending on the direction, longitudinal position, and radial growth rate and could be drawn in general as follows. The shrinkage in the tangential direction of all categorized trees tends to increase from the pith to the bark, except at the bottom of slow- and average-growth trees, showing a tendency to decrease toward the bark. For the shrinkage in the radial direction, the fast-growth tree tends to increase toward the bark, while the slow- and average-growth trees tend to decrease and increase toward the bark, respectively. In the case of the shrinkage in the longitudinal direction, all the categorized trees tend to decrease or remain constant toward the bark.

Similarly, the table described that the variations in the longitudinal direction varied depending on the direction, radial growth rate, and radial position. In general, the results show that the shrinkage in the tangential direction of the slow- and average-growth trees tends to decrease, while the fast-growth tree tends to increase toward the top of the tree. For the shrinkage in the radial direction, each categorized tree seems to have different patterns, showing a tendency to remain constant, decrease, and increase toward the top of the slow-, average-, and fast-growth trees, respectively. In the case of the shrinkage in the longitudinal direction, the slow-growth tree tends to decrease, while the average- and fast-growth trees tend to increase toward the top of the trees.

As predicted, the shrinkage of all the categorized trees in the tangential direction was the highest compared to the other directions. In this study, the average shrinkage in the tangential direction was 3.03, 3.19, and 3.85% for slow-, average-, and fast-growth trees, respectively. The average shrinkage in the radial direction was 1.83, 1.79, and 2.41% for slow-, average-, and fast-growth trees, respectively. In addition, average shrinkage in the longitudinal direction was 0.53, 0.61, and 0.82% for slow-, average-, and fast-growth trees, respectively. The results were much higher than the previous studies, mentioning that the shrinkage in the tangential and radial directions was 1.2–2.7 and 0.5–1.8%, respectively (Nordahlia et al., 2013).

Although the fast-growth tree has a lower air-dry density, the results showed that the wood has higher shrinkage in all directions than the other categorized trees. As wood density indicates the cell wall substance in wood, it is reasonable to assume that shrinkage is closely associated with density. Nonetheless, several studies have reported that density less or moderately affects shrinkage (Saranpaa, 1992; Zhang et al., 1994). The strong correlation between shrinkage and juvenile wood is also anticipated, given that juvenile wood typically features a larger microfibril angle in the S_2 layer of the cell wall, resulting in more significant shrinkage than mature wood, particularly in the longitudinal direction. Therefore, the results suggested that the fast-growth tree has more juvenile wood than the other categorized trees. The other factors, such as extractive content, probably have a more significant effect on the shrinkage as it was reported that the extractive in the cell walls reduces the hygroscopicity of wood (Choong & Achmadi, 1989), suggesting that the fast-growth tree has less extractive content than the other categorized trees. However, further study is required to investigate the presence and distribution of juvenile wood as well as the extractive content of all the categorized trees, including their effects on shrinkage.

Table 4.3: Shrinkage variations in the radial and longitudinal directions of all the categorized trees at an MC of 12%.

Tree categorize	Longitudinal Position	Distance from the pith (mm)	Shrinkage (%)		
			Tangential	Radial	Longitudinal
Slow-growth tree	Bottom	0–20	4.11	2.14	0.43
		20–40	3.16	2.06	0.68
		40–60	3.62	2.04	0.56
		60–80	3.52	1.65	0.57
		80–100	2.87	1.66	0.62
		100–120	2.71	1.75	0.51
		120–140	3.28	1.81	0.57
	Breast height	0–20	-	-	-
		20–40	2.58	1.60	0.73

		40–60	3.03	1.81	0.62
		60–80	3.04	1.70	0.68
		80–100	2.72	1.98	0.53
		100–120	2.64	1.83	0.56
	Middle	0–20	-	-	-
		20–40	3.02	1.89	0.69
		40–60	3.13	2.00	0.40
		60–80	3.20	1.76	0.48
		80–100	3.18	1.80	0.40
		100–120	3.60	1.79	0.55
	Top	0–20	-	-	-
		20–40	2.53	1.70	0.38
		40–60	2.59	1.96	0.45
		60–80	3.13	1.81	0.42
Average-growth tree	Bottom	0–20	-	-	-
		20–40	4.99	2.32	0.52
		40–60	3.94	2.22	0.65
		60–80	3.58	1.93	0.54
		80–100	-	-	-
		100–120	3.21	1.94	0.47
		120–140	2.25	1.86	0.58
	Breast height	0–20	-	-	-
		20–40	3.38	1.67	0.47
		40–60	3.70	1.40	0.49
		60–80	2.71	1.50	0.79
		80–100	3.13	1.94	0.72
		100–120	2.62	1.60	0.59
		120–140	3.56	1.89	0.68
	Middle	0–20	-	-	-
		20–40	2.80	1.74	0.62
		40–60	3.24	1.73	0.68
		60–80	3.07	1.57	0.71
		80–100	2.60	1.52	0.64
		100–120	2.80	1.65	0.74

		120–140	3.36	1.75	0.76
		140–160	3.55	1.79	0.62
	Top	0–20	-	-	-
		20–40	2.67	1.71	0.57
		40–60	2.78	1.78	0.60
		60–80	3.28	1.77	0.53
Fast-growth tree	Bottom	0-20	-	-	-
		20–40	3.34	1.91	0.84
		40–60	3.71	2.01	0.63
		60–80	3.80	2.04	0.73
		80–100	2.04	1.79	0.75
		100–120	-	-	-
		120–140	-	-	-
		140–160	3.02	2.18	0.69
		160–180	4.16	2.18	0.78
		180–200	5.28	2.46	0.88
	Breast height	0–20	-	-	-
		20–40	-	-	-
		40–60	3.64	2.18	0.86
		60–80	3.67	2.29	1.04
		80–100	4.32	2.40	1.06
		100–120	3.41	2.38	0.85
		120–140	-	-	-
		140–160	3.15	2.47	0.98
		160–180	5.94	2.35	0.82
		180–200	4.65	2.35	1.04
	Middle	0–20	-	-	-
		20–40	-	-	-
		40–60	2.58	1.45	0.81
		60–80	3.99	2.91	1.25
		80–100	3.52	3.01	0.79
		100–120	5.89	3.75	0.80
		120–140	4.72	3.32	0.80
		140–160	6.26	4.17	0.92

	160–180	5.43	2.97	0.69
	0–20	-	-	-
	20–40	-	-	-
	40–60	2.72	2.04	0.79
Top	60–80	2.76	2.10	0.69
	80–100	2.99	1.99	0.71
	100–120	3.39	2.40	0.68
	120–140	3.34	2.15	0.68

Note: - is the measurement was not conducted.

4.3 Mechanical Properties

4.3.1 Bending Strength Properties

Figure 4.6 illustrates the MOR variations in the radial and longitudinal directions of all the categorized trees. The results described that the radial variation in the MOR of all the categorized trees has a typical pattern, exhibiting an increase toward the bark. A gradual increase in the MOR was observed in the average- and fast-growth trees, while a rapid increase was observed in the slow-growth tree.

On the other hand, the figure showed that the MOR variations in the longitudinal direction have varied patterns depending on the radial growth rate and radial position. The slow-growth tree tends to have a constant MOR, while the MOR of the average- and fast-growth trees tend to increase toward the top of the trees. Although the top of the tree typically contains more juvenile wood, which often possesses lower strength properties than mature wood, the figure showed that the top of the average- and fast-growth trees tend to have a higher MOR, probably due to its higher density.

Figure 4.7 illustrates the MOE variations in the radial and longitudinal directions of all the categorized trees. In general, the figure demonstrated that the radial variation in the MOE has a similar tendency to the MOR, exhibiting an increase toward the bark. An increase in the MOR and MOE in the radial direction is understandable because the wood density also increases from the pith toward the bark. It is well known that wood density positively affects the bending properties.

In addition, the figure described that the MOE variations in the longitudinal direction of all the categorized trees have a typical tendency, showing an increase toward the top of the trees. Similar to the MOR, the top of all the categorized trees tends to have a higher MOE, which could be attributed to its higher density.

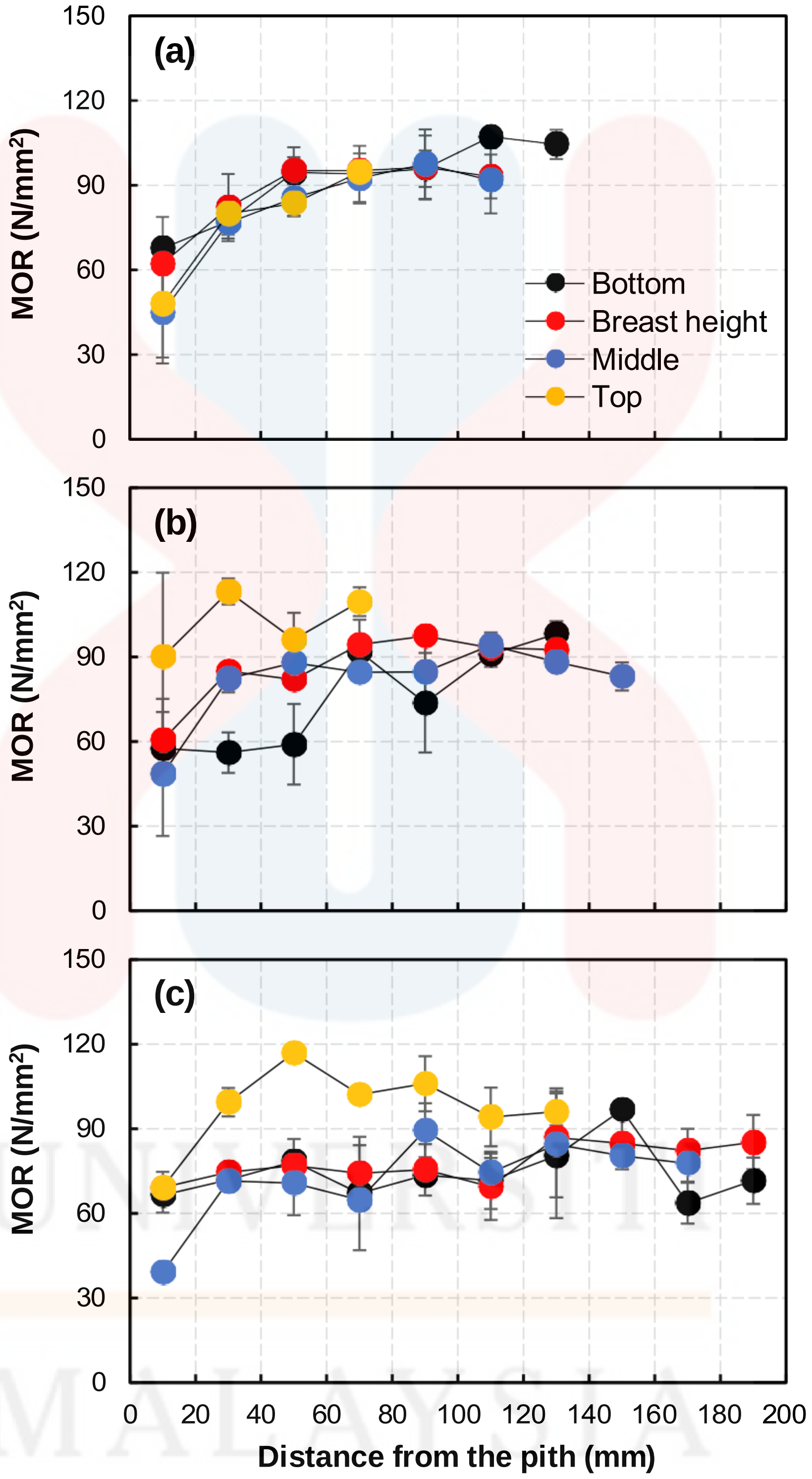

Figure 4.6: MOR variations in the radial and longitudinal directions of the slow- (a), average- (b), and fast-growth (c) trees.

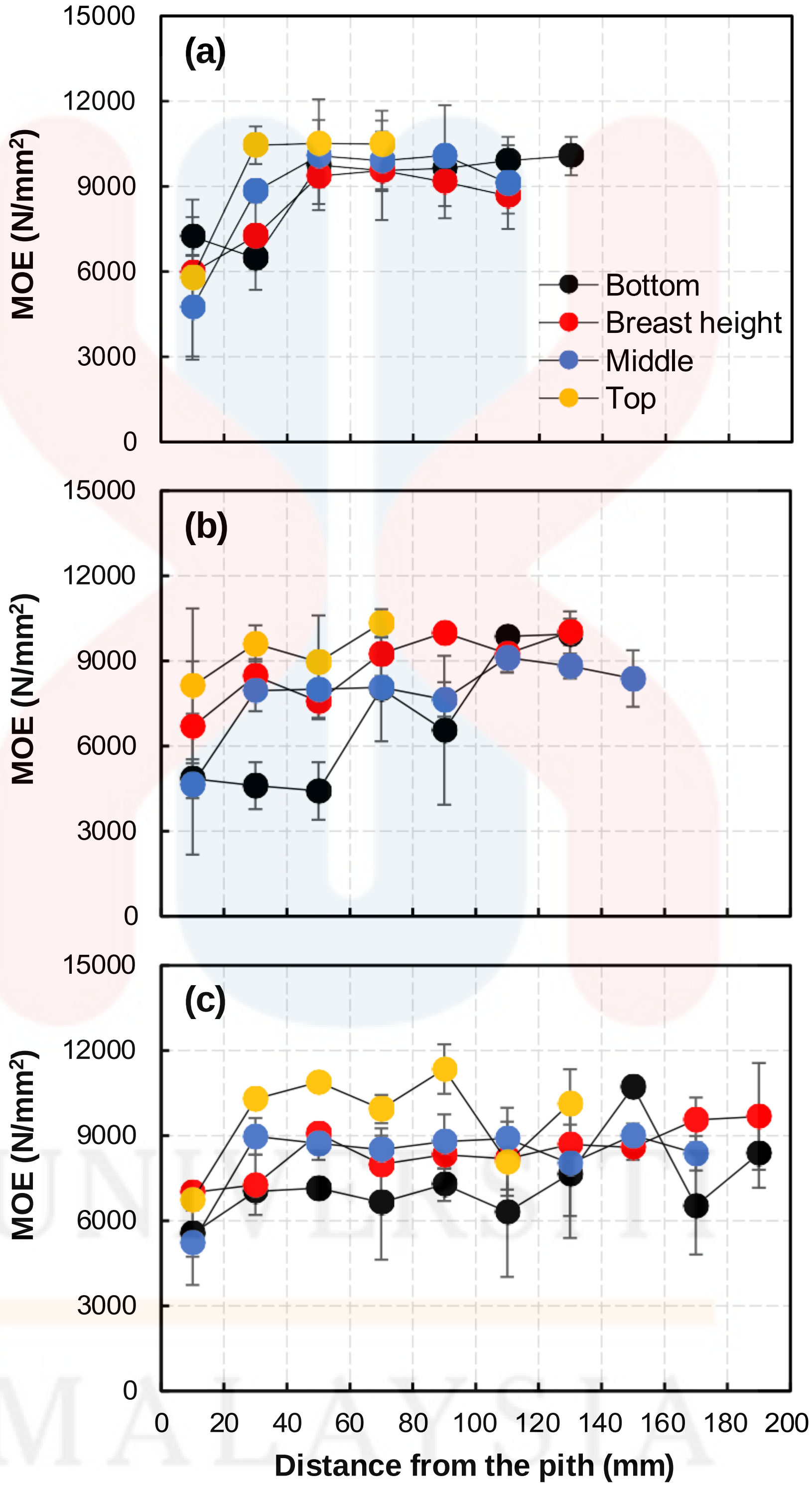

Figure 4.7: MOE variations in the radial and longitudinal directions of the slow- (a), average- (b), and fast-growth (c) trees.

In this study, the MOR and MOE of slow-, average-, and fast-growth trees were 85.2 and 8,811, 84.4 and 8,043, and 79.3 and 8,314 N/mm^2, respectively, indicating that the fast-growth tree tends to have a lower MOR and MOE, probably due to a relatively lower density than the other categorized trees. In addition, a lower value was obtained from the previous study, mentioning that the average MOR and MOE of sentang were 60.0–83.9 and 6,770–6,862 N/mm^2, respectively (Noraini, 1997).

4.3.2 Compression Strength

Figure 4.8 illustrates the compression strength variations in the radial and longitudinal directions of all the categorized trees. The results showed that the radial variation in the compression strength of all the categorized trees has a typical pattern, increasing gradually until maximum strength is reached and then slightly decreasing toward the bark. A relatively similar result with the MOR and MOE, the density affects an increase in the compression strength in the radial direction.

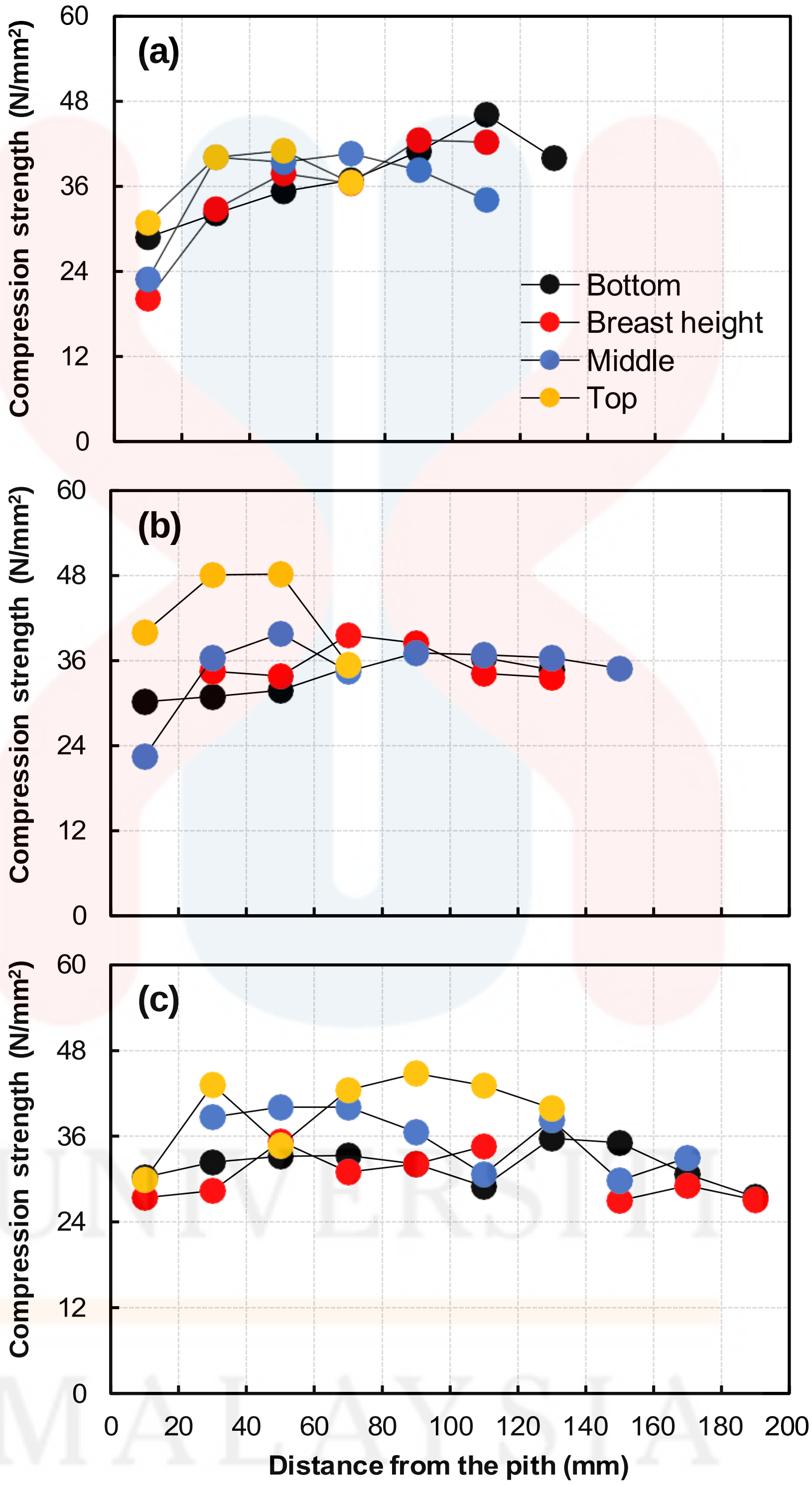

Figure 4.8: Compression strength variations in the radial and longitudinal directions of the slow- (a), average- (b), and fast-growth (c) trees.

In addition, the compression strength variations in the longitudinal direction tend to increase toward the top of all the categorized trees, except for the fast-growth tree, showing a decrease from the bottom to the breast height, followed by an increase toward the top of the tree. Similar to the MOR and MOE, the top of all the categorized trees tends to have a higher compression strength due to their higher density.

In this study, the average compression strength of slow-, average-, and fast-growth trees was 36.3, 35.9, and 34.0 N/mm^2, respectively, indicating that the fast-growth tree tends to have a lower compression strength than the other categorized trees. Similar to MOR and MOE, this is probably due to a relatively lower density of the fast-growth tree. In addition, a comparable result was obtained from the previous study that reported the average compression strength of sentang was 31.0–42.0 N/mm^2 (Noraini, 1997).

CHAPTER 5

CONCLUSIONS AND FUTURE WORK

5.1 Conclusions

This study investigated the effect of radial growth rate on the anatomical, physical, and mechanical properties variations in the radial and longitudinal directions of the 26-year-old sentang tree planted in Jeli, Kelantan, Malaysia. For these purposes, the trees were categorized into slow-, average-, and fast-growth based on their DBH, and the properties variations from the pith to the bark and from the bottom to the top of the trees were examined.

The results revealed that despite the differences in the radial growth rate, radial variation in the vessel element length and diameter, air-dry density, MOR, MOE, and compression strength tend to have a typical pattern, experiencing an increase from the pith to the bark. In comparison, radial variation in the fiber length and diameter, green density, and shrinkage were found to have varied patterns depending on the radial growth rate and longitudinal position.

On the other hand, longitudinal variation in the fiber and vessel element dimensions tended to have varied patterns depending on the radial growth rate and radial position. Regarding the physical properties, except for the shrinkage, longitudinal variation in the MC and density was found to have a typical pattern despite the differences in the radial growth rate. The green MC experiences a decrease from the bottom to the top, while the density tends to increase toward the top of the trees. Similarly, longitudinal variation in the mechanical properties tended to have a typical pattern of an increase toward the top of the trees despite the differences in the radial growth rate.

In addition, the radial growth rate seems to affect the wood properties in general. The slow-growth tree tends to have a shorter fiber length and smaller fiber diameter, reflecting a considerably higher wood density, and thus has the highest mechanical properties. In contrast, the fast-growth tree tends to have a lower wood density and thus has the lowest mechanical properties than the other categorized trees.

5.2 Future Work

This research has revealed the effect of radial growth rate on the wood properties of sentang trees planted in Jeli, Kelantan. As the wood has adequate properties and could be used as raw materials for various end-products, future studies on the effect of site locations on the wood properties of sentang should be considered. Therefore, more extensive samples from trees planted at different sites with different geographical and environmental characteristics must be studied. The interaction between site locations and radial growth rate must be further elaborated to draw general conclusions regarding the properties of sentang planted in Malaysia.

REFERENCES

Adi D.S., Risanto, L., Damayanti, R., Rullyati, S., Dewi, L.M., Susanti, R., Dwianto, W., Hermiati, E., & Watanabe, T. (2014). Exploration of Unutilized Fast Growing Wood Species from Secondary Forest in Central Kalimantan: Study on the Fiber Characteristic and Wood Density. Procedia Environmental Sciences, 20, 321–327.

Atiqah, A.H., Rhyma, P.P., Jamhuri, J., Zulfa, A.W., Samsinar, M.S., & Norizah, K. (2020). Using Google Earth imagery to detect distribution of forest cover change-Is the technique practical for Malaysian forests? The Malaysian Forester, 83(1), 1–15.

Azmi, A., Ahmad, Z., Lum, W.C., Baharin, A., Za'ba, N.I.L., Bhkari, N.M., & Lee, S.H. (2022). Compressive Strength Characteristic Values of Nine Structural Sized Malaysian Tropical Hardwoods. Forests, 13(8), 1172.

Babiak, M., & Kúdela, J. (1995). A contribution to the definition of the fiber saturation point. Wood Science and Technology, 29(3), 217–226.

Bahtiar, E.T, Kim, N.H. & Iswanto A.H. (2023). Biological Rotation Age of Community Teak (*Tectona grandis*) Plantation Based on the Volume, Biomass, and Price Growth Curve Determined through the Analysis of Its Tree Ring Digitization. Forests, 14(10), 1944.

Barnett, J.R., & Bonham, V.A. (2004). Cellulose microfibril angle in the cell wall of wood fibres. Biological Reviews, 79(2), 461–472.

Baviskar, S.N. (2011). A Quick & Automated Method for Measuring Cell Area using ImageJ. The American Biology Teacher, 73(9), 554–556.

Bernardes, R.C., Barbosa, W.F., Martins, G.F., & Lima, M.A.P. (2018). The reduced-risk insecticide azadirachtin poses a toxicological hazard to stingless bee *Partamona helleri* (Friese, 1900) queens. Chemosphere, 201, 550–556.

Borrega, M., & Gibson, L.J. (2015). Mechanics of balsa (*Ochroma pyramidale*) wood. Mechanics of Materials, 84, 75–90.

Carle, J., Vuorinen, P., & Del Lungo, A. (2002). Status and trends in global forest plantation development. Forest Products Journal, 52(7/8), 12–23.

Carino, H.F., & Biblis, E.J. (2009). Impact of stand density on the quality and value of 35-year-old loblolly pine plantation sawtimber: A case study. Forest Products Journal, 59(3), 62–66.

Carrasco, L.O., Bucci, S.J., di Francescantonio, D., Lezcano, O.A., Campanello, P.I., Scholz, F.G., Rodríguez, S., Madanes, N., Cristiano, P.M., Hao, G.Y., & Holbrook, N.M. (2014). Water storage dynamics in the main stem of subtropical tree species differing in wood density, growth rate and life history traits. Tree Physiology, 35(4), 354–365.

Choong, E.T., & Achmadi, S.S. (1999). Effect of Extractives on Moisture Sorption and Shrinkage in Tropical Woods. Wood and Fiber Science, 23(2), 185–196.

Chowdhury, M.Q., Ishiguri, F., Iizuka, K., Takashima, Y., Matsumoto, K., Hiraiwa, T., Ishido, M., Sanpe, H., Yokota, S., & Yoshizawa, N. (2009). Radial variations of wood properties in *Casuarina equisetifolia* growing in Bangladesh. Journal of Wood Science, 55 (2), 139–143.

Dadzie, P.K., & Amoah, M. (2015). Density, some anatomical properties and natural durability of stem and branch wood of two tropical hardwood species for ground applications. European Journal of Wood and Wood Products, 73(6), 759–773.

Dias, A., Gaspar, M.J., Carvalho, A., Pires, J., Lima-Brito, J., Silva, M.E., & Louzada, J.L. (2018). Within-and between-tree variation of wood density components in Pinus nigra at six sites in Portugal. Annals of Forest Science, 75(2), 1–19.

Elustondo, D. (2010). Lumber quality model: The theory. Wood Material Science and Engineering, 5(3–4), 162–172.

Evans, J. (1999). Sustainability of forest plantations: a review of evidence and future prospects. The International Forestry Review, 1(3), 153–162.

Evans, J.W., Senft, J.F., & Green, D.W. (2000). Juvenile wood effect in red alder: analysis of physical and mechanical data to delineate juvenile and mature wood zones. Forest Products Journal, 50(7/8), 75-87.

FAO (2002). Case study of tropical forest plantations in Malaysia by D.B.A Krishnapillay. Forest Plantations Working Paper 23. Forest Resources Development Service, Forest Resources Division. FAO, Rome (unpublished).

FAO (2020). Global Forest Resources Assessment 2020: Main report. Rome. https://doi.org/10.4060/ca9825en. Accessed on October 02, 2022.

Feist, W.C., & Tarkow, H. (1967). A new procedure for measuring fiber saturation points.

Forest Products Journal, 17(10), 65–68.

Forestry Department Peninsular Malaysia (2007). FDPM Annual Report 2007. https://www.forestry.gov.my/images/Laporan%20Tahunan/2007/ANNUAL%20REPORT%20JPSM%202007.PDF. Accessed on October 02, 2022.

Forestry Department Peninsular Malaysia (2008). FDPM Annual Report 2008. https://www.forestry.gov.my/images/Laporan%20Tahunan/2008/FINAL%20LAYOUT%20JPSM%202008.pdf. Accessed on October 02, 2022.

Forestry Department Peninsular Malaysia (2009). FDPM Annual Report 2009. https://www.forestry.gov.my/images/Laporan%20Tahunan/2009/annual%20report%20perhutanan%202009.pdf. Accessed on October 02, 2022.

Forestry Department Peninsular Malaysia (2010). FDPM Annual Report 2010. https://www.forestry.gov.my/images/Laporan%20Tahunan/2010/A.R%20PERHUTANAN%202010_090911_full.pdf. Accessed on October 02, 2022.

Forestry Department Peninsular Malaysia (2011). FDPM Annual Report 2011. https://www.forestry.gov.my/images/Laporan%20Tahunan/2011/LaporanTahunanJPSM2011.pdf. Accessed on October 02, 2022.

Forestry Department Peninsular Malaysia (2012). FDPM Annual Report 2012. https://www.forestry.gov.my/images/Laporan%20Tahunan/2012/LaporanTahunanJPSM2012.pdf. Accessed on October 02, 2022.

Forestry Department Peninsular Malaysia (2013). FDPM Annual Report 2013. https://www.forestry.gov.my/images/Laporan%20Tahunan/2013/laporantahunan2013.pdf. Accessed on October 02, 2022.

Forestry Department Peninsular Malaysia (2014). FDPM Annual Report 2014. https://www.forestry.gov.my/images/Laporan%20Tahunan/2014/LaporanTahunan2014.pdf. Accessed on October 02, 2022.

Forestry Department Peninsular Malaysia (2015). FDPM Annual Report 2015. https://www.forestry.gov.my/images/Laporan%20Tahunan/2015/LaporanTahunan2015.pdf. Accessed on October 02, 2022.

Forestry Department Peninsular Malaysia (2016). FDPM Annual Report 2016. https://www.forestry.gov.my/images/Laporan%20Tahunan/2016/annual-report-jpsm-2016.pdf. Accessed on October 02, 2022.

Forestry Department Peninsular Malaysia (2017). FDPM Annual Report 2017. https://www.forestry.gov.my/images/Laporan_Tahunan/2017/Laporan_Tahunan_2017.pdf. Accessed on October 02, 2022.

Forestry Department Peninsular Malaysia (2018). FDPM Annual Report 2018. https://www.forestry.gov.my/images/Laporan_Tahunan/2018/ARJPSM2018.pdf. Accessed on October 02, 2022.

FPDSB (2018). Minutes of Meeting on January 16, 2018: Physical Progress of Forest Plantation Development Programme (2). Ministry of Primary Industries and Commodities, Putrajaya, Malaysia.

Freezailah, C.Y., & Fielding, J.M. (1971). The Development and results of the pilot plantation project and prospects for the future. FO: SF/MAL/12. Working Paper No.18. FAO, Rome.

Gan, K.S., Choo, K.T., & Lim, S.C. (1999). Timber Notes-Light Hardwoods VII: Sentang, Sepetir, Sesendok, Terap, Terentang. Timber Technology Bulletin No. 17 Forest Research Institute Malaysia, Kuala Lumpur, Malaysia.

GBIF Secretariat (2021). GBIF Backbone Taxonomy. Checklist dataset https://doi.org/10.15468/39omei. Accessed via https://www.gbif.org/species/3852944 on October 03, 2022.

Green, D.W., Winandy, J.E., & Kretschmann, D.E. (1999). Mechanical Properties of Wood. In Wood Handbook: Wood as an Engineering Material. General Technical Report FPL, GTR-113. Forest Products Laboratory, Madison, USA.

Günter, S., Weber, M., Stimm, B., and Mosandl, R. (eds). (2011). Silviculture in the Tropics. Springer-Verlag, New York, USA.

Hashim, M.N., Hazim, M., & Syafinie, A.M. (2015). Strategic forest plantation establishment in Malaysia for future product development and utilization. Proceeding of Kuala Lumpur International Agriculture, Forestry and Plantation Conference, September 12–13, 2015, Kuala Lumpur.

Hermawan, A., Sakagami, H., Ahmad Sobri, S., Mohamad Amini, M.H., Mhd. Ramle, S.T., & Rasid, S. (2020). The effects of drying temperatures on preservative retention and penetration of some Malaysian fast-growing species timbers. Drying Technology, 39(4), 1–10.

Hidayati, F., Ishiguri, F., Makino, K., Tanabe, J., Aiso, H., Prasetyo, V.E., Marsoem, S.N., Wahyudi, I., Iizuka, K., & Yokota, S. (2017). The effects of radial growth rate on wood properties and anatomical characteristics and an evaluation of the xylem maturation process in a tropical fast-growing tree species, *Gmelina arborea*. Forest Products Journal, 67(3-4), 297–303.

Honjo, K., Furukawa, I., & Sahri, M.H. (2005). Radial variation of fiber length increment in Acacia mangium. IAWA Journal, 26(3), 339–352.

Hossain, N., & Jalil, R. (2018). Analyses of bio-energy properties from Malaysian local plants: sentang and sesendok. Asia Pacific Journal of Energy and Environment, 5(1), 7–10.

Huat, O.K., Tsai, L.M., Kadir, J., & Awang, K. (2003). Some effects of site on the growth of *Azadirachta excelsa* (Jack) Jacobs in Peninsular Malaysia. Proceeding of the XII World Forestry Congress, September 21–28, 2003, Quebec.

Hummel, H.E., Langner, S.S., Hein, D.F., Sanguanpong, U., & Schmutterer, H. (2016). Unusually versatile plant genus Azadirachta with many useful and so far incompletely exploited properties for agriculture, medicine and industry. Acta Fytotechnica et Zootechnica, 18(5), 1269–175.

Isman, M.B., Koul, O., Luczynski, A., & Kaminski, J. (1990). Insecticidal and antifeedant bioactivities of neem oils and their relationship to azadirachtin content. Journal of Agricultural and Food Chemistry, 38(6), 1406–1411.

Iswanto, A.H., Febrianto, F., & Wahyudi, I. (2010). Basic Properties Of Sentang Wood (*Melia Excelsa* Jack) and Its Suitability as Oriented Strand Board Materials. Perennial, 6(2), 79–82.

Jacobs, M. (1961). *Azadirachta excelsa* (Jack). Gardens' Bulletin Singapore, 18:75.

JIS Z2101 (2009). Methods of test for woods. Japan Standards Association.

Jankowska, A., Drożdżek, M., Sarnowski, P., & Horodeński, J. (2017). Effect of extractives on the equilibrium moisture content and shrinkage of selected tropical wood species. BioResources, 12(1), 597–607.

Jett, J.B., & Zobel B.J. (1975). Wood and pulping properties of young hardwoods. TAPPI Journal, 58(1), 92–96.

Kaewnang-O, E., Ngampongsai, A., Subhadhirasakul, S., & Srichana, T. (2011). Toxicity of fixed oil and crude extract from sa-dao-thiam, *Azadirachta excelsa* (Jack) seed kernel to *Aedes aegypti* (L.). Songklanakarin Journal of Science & Technology, 33(1), 43–49.

Kang, C.W., Lee, Y.H., Kang, H.Y., Kang, W., Xu, H., & Chung, W.Y. (2011). Radial Variation of Sound Absorption Capability in the Cross Sectional Surface of Yellow Poplar Wood. Journal of the Korean Wood Science and Technology, 39(4), 326–32.

Kang, H., Wen, X., Deng, X., Chen, L., & Xiao, F. (2021). Heartwood and Sapwood Variation and Development in Chenshan Red-Heart Chinese Fir (*Cunninghamia lanceolata* (Lamb.) Hook). Forest Products Journal, 71(4), 299–308.

Kanowski, P. (2001). Resource Management in Asia-Pacific. Working Paper No. 6: Afforestation and plantation forestry. The Australian National University, Canberra, Australia.

Karlsson, L., Mörling, T., & Bergsten, U. (2013). Influence of silvicultural regimes on the volume and proportion of juvenile and mature wood in boreal Scots pine. Silva Fennica, 47(4), 1–17.

Kijkar, S., & Boontawee, B. (1995). *Azadirachta excelsa* (Jack) Jacobs: A lesser Known Species. ASEAN Tree Seed Center Project, Review Paper No. 3. Muak-Lek, Saraburi, Thailand.

Kim, N.T., Matsumura, J., Oda, K., & Cuong, N.V. (2009). Possibility of improvement in fundamental properties of wood of acacia hybrids by artificial hybridization. Journal of Wood Science, 55(1), 8–12.

Korkmaz, O., & Büyüksarı, Ü. (2019). Effects of moisture content on mechanical properties of micro-size oak wood. BioResources, 14(4), 7655–7663.

Kurose, K. & Yatagai, M. (2005). Components of the essential oils of *Azadirachta indica* A. Juss, *Azadirachta siamensis* Velton, and *Azadirachta excelsa* (Jack) Jacobs and their comparison. Journal of Wood Science, 51(2), 185–188.

Larsson, P.T., Lindström, T., Carlsson, L.A., & Fellers, C. (2018). Fiber length and bonding effects on tensile strength and toughness of kraft paper. Journal of Materials Science 53(3), 3006–3015.

Lim, S.C., Can K.S., & Khairul A. (2006). Timber of Sentang. Timber Technology Bulletin No. 38. Forest Research Institute Malaysia, Kuala Lumpur, Malaysia.

Mabberly, D.J., & Pannell, C.M. (1989). Meliaceae in Whitmore, T.C., Ng, F.S.P. (eds).

Tree Flora of Malaya: A Manual for Foresters, Volume 4. Longman, Kuala Lumpur.

Mabberley, D.J., Pannell, C.M., Sing, A.M. (1995). Flora Malesiana, Series 1: Spermatophyta (Seed Plants). Volume 12, Part 1: Meliaceae. National Herbarium of the Netherlands, the Netherlands.

Machado, J.S., Louzada, J.L., Santos, A.J., Nunes, L., Anjos, O., Rodrigues, J., Simões R.M.S., & Pereira, H. (2014). Variation of wood density and mechanical properties of blackwood (*Acacia melanoxylon* R. Br.). Materials & Design, 56, 975–980.

Mak-Mensah, E.E., & Firempong, C.K. (2011). Chemical characteristics of toilet soap prepared from neem (*Azadirachta indica* A. Juss) seed oil. Asian Journal of Plant Science and Research, 1(4), 1–7.

McDonald, S.S., Williamson, G.B., & Wiemann, M.C. (1995). Wood specific gravity and anatomy in *Heliocarpus appendiculatus* (Tiliaceae). American Journal of Botany, 82(7), 855-861.

Mendoza, R.C., Daracan, V.C., Manalo, R.D., Batallones, C.H.R., Jaurigue, K.G., Romano, A.D., & Abasolo, W.P. (2019). Anatomical and physico-mechanical characterization of narra (*Pterocarpus indicus* Willd.) branchwood collected in Mount Makiling Forest Reserve, Laguna, Philippines. Philippine Journal of Science, 148(4), 705–713.

Menon, P.K.B., Sulaiman, A., & Lim S.C. (2004). Structure and Identification of Malayan Woods. Malayan Forest Record No. 25. Forest Research Institute Malaysia, Kuala Lumpur, Malaysia.

Mitchell, P. H. (2018). Calculating the equilibrium moisture content for wood based on humidity measurements. BioResources, 13(1), 171–175.

MTIB (2019). Annual Report of the Malaysian Timber Industry Board 2019. https://www.mtib.gov.my/en/annual-report. Accessed on October 02, 2022.

Muñoz, F., & Moya, R. (2008). Moisture content variability in kiln-dried *Gmelina arborea* wood: Effect of radial position and anatomical features. Journal of Wood Science, 54 (4), 318–322.

Naji, H.R., Sahri, M.H., Nobuchi, T., & Bakar, E.S. (2013). Radial variation of wood cell features under different stocking densities management of two new clones of rubberwood (*Hevea brasiliensis*). Journal of Wood Science, 59, 460–468.

Niklas, K.J., & Spatz, H.C. (2010). Worldwide correlations of mechanical properties and green wood density. American Journal of Botany, 97(10), 1587–1594.

Noraini, A. (ed). (1997). *Azadirachta excelsa*: a monograph. Research Pamphlet No. 120. Forest Research Institute Malaysia, Kuala Lumpur, Malaysia.

Nordahlia, A.S., Ani, S., Zaidon, A., & Hamami, S.M. (2011). Fibre morphology and physical properties of 10-year-old sentang (*Azadirachta excelsa*) planted from rooted cuttings and seedlings. Journal of Tropical Forest Science, 23(2), 222–227.

Nordahlia, A.S., Hamdan, H., & Anwar, U.M.K. (2013). Wood properties of selected plantation species: *Khaya ivorensis* (African mahogany), *Azadirachta excelsa* (sentang), *Endospermum malaccense* (sesendok) and *Acacia mangium*. Timber Technology Bulletin No. 51, Forest Research Institute Malaysia, Kuala Lumpur, Malaysia.

Nordahlia, A.S., Anwar, U.M.K., Hamdan, H., Zaidon, A., & Omar, M.M. (2014). Mechanical properties of 10-year-old sentang (*Azadirachta excelsa*) grown from vegetative propagation. Journal of Tropical Forest Science, 26 (2), 240–248.

Ofori, J., & Brentuo, B. (2005). Green moisture content, basic density, shrinkage and drying characteristics of the wood of Cedrela odorata grown in Ghana. Journal of Tropical Forest Science, 17(2), 211–223.

Olson, M., Rosell, J.A., Martínez-Pérez, C., León-Gómez, C., Fajardo, A., Isnard, S., Cervantes-Alcayde, M.A., Echeverría, A., Figueroa-Abundiz, V.A., Segovia-Rivas, A., Trueba, S., & Vázquez-Segovia, K. (2020). Xylem vessel-diameter‑shoot-length scaling: ecological significance of porosity types and other traits. Ecological Monographs, 90(3), e01410.

Orwa, C., Mutua, A., Kindt, R., Jamnadass, R.H., & Simons, A. (2009). Agroforestree Database: a tree reference and selection guide version 4.0.

Premono, B.T., Lestari, S., & Winarno, B. (2019). Tree-crop diversification by smallholder farmers in Southern Sumatra to diversify sources of income. IOP Conference Series: Earth and Environmental Science, 298, 012032.

Przybysz, K., Malachowska, E., Martyniak, D., Boruszewski, P., Iłowska, J., Kalinowska, H., & Przybysz, P. (2018). Yield of pulp, dimensional properties of fibers, and properties of paper produced from fast growing trees and grasses. BioResources 13(1), 1372–1387.

Rafeadah, R., & Rahim, S. (2007). Chemical and physical properties of juvenile Acacia hybrid and *Azadirachta excelsa*. Journal of the Institute of Wood Science, 17(5), 290–294.

Rahmawathi, A.M., Wijayanto, N., & Wulandari, A.S. (2017). Short Communication: Growth analysis of sentang (*Azadirachta excelsa*) in agroforestry system. Biodiversitas, 18, 589–592.

Ratnasingam, J. (2019). Status and challenges of plantation forestry in Malaysia: a cost-benefit analysis. Report for the Investment Unit of Malayan Banking Group Berhad, Kuala Lumpur, Malaysia.

Ratnasingam, J., Latib, H.A., Paramjothy, N., Liat, L.C., Nadarajah, M., & Ioras, F. (2020). Plantation forestry in Malaysia: an evaluation of its successes and failures since the 1970. Notulae Botanicae Horti Agrobotanici Cluj-Napoca, 48(4), 1789–1801.

Ruddin, N.Z.H.M., Rasid, S., & Hermawan, A. (2020). Drying properties of Sentang (*Azadirachta excelsa*) dried under different temperatures. IOP Conference Series: Earth and Environmental Science, 596, 012034.

Ruffinatto, F., Crivellaro, A., & Wiedenhoeft, A. (2015). Review of macroscopic features for hardwood and softwood identification and a proposal for a new character list. IAWA Journal, 36, 208–241.

Ruffinatto, F., & Crivellaro, A. (2019). Atlas of macroscopic wood identification: with a special focus on timbers used in Europe and CITES-listed species. Springer Nature.

Saranpää, P. (1992). Basic density, longitudinal shrinkage and tracheid length of juvenile wood of *Picea abies* (L.) Karst. Scandinavian Journal of Forest Research, 9, 69–74.

Saranpää, P. (2003). Wood density and growth. Wood quality and its biological basis. In Barnett, J.R., & Jeronimidis, G. (eds). Wood Quality and its Biological Basis. Blackwell Publishing Ltd, Oxford, UK.

Schulgasser, K., & Witztum, A. (2015). How the relationship between density and shrinkage of wood depends on its microstructure. Wood Science and Technology, 49(2), 389–401.

Selvaraj, P., & Muhammad, A.B. (1980). A checklist of plantation trials in Peninsular Malaysia. Research Pamphlet No. 79. Forest Research Institute Malaysia, Kuala Lumpur, Malaysia.

Shmulsky, R., & Jones, P.D. (2019). Forest products and wood science: An introduction (7th ed). John Wiley & Sons Ltd. Hoboken, USA.

Simpson, W.T. (1971). Equilibrium moisture content prediction for wood. Forest Products Journal, 21(5), 48–49.

Simpson, W.T., & TenWolde, A. (1999). Physical Properties and Moisture Relations of Wood. In Wood Handbook: Wood as an Engineering Material. General Technical Report FPL, GTR-113. Forest Products Laboratory, Madison, USA.

Song, K., Yin, Y., Salmén, L., Xiao, F., & Jiang, X. (2014). Changes in the properties of wood cell walls during the transformation from sapwood to heartwood. Journal of Materials Science, 49(4), 1734–1742.

Tomczak, K., Tomczak, A., Naskrent, B., & Jelonek, T. (2021). The radial gradient of moisture content of Silver Birch wood in different seasons. Silva Fennica, 55 (3), 10545.

Trockenbrodt, M., Misalam, K., & Lajanga, J. (1999). Physical and elasto-mechanical wood properties of young Sentang (*Azadirachta excelsa*) planted in Sabah, Malaysia. Holz als Roh-und Werkstoff, 57(3), 210–214.

Wahyudi, I., Ishiguri, F., Makino, K., Aiso, H., Takashima, Y., Ohshima, J., Iizuka, K., & Yokota, S. (2016). Evaluation of xylem maturation and the effects of radial growth rate on anatomical characteristics and wood properties of *Azadirachta excelsa* planted in Indonesia. Journal of the Indian Academy of Wood Science, 13(2), 138–144.

Wan Mohamed, W., Baharum, A., Ahmad, I., Abdullah, I., & Zakaria, N.E. (2018). Effects of fiber size and fiber loading on mechanical properties and morphology of thermoplastic mengkuang reinforced natural rubber composites. BioResources 13(2), 2945–2959.

Wang, Y., Zhang, R., & Zhou, Z. (2021). Radial variation of wood anatomical properties determines the demarcation of juvenile-mature wood in *Schima superba*. Forests, 12, 512.

Wong, T.M., Lim, S.C., & Chung, R.C.K. (2002). A dictionary of Malaysian timbers. Malayan Forest Records No. 30. Forest Research Institute Malaysia, Kuala Lumpur, Malaysia.

Winandy, J. E., & Rowell, R. M. (2012). Chemistry of Wood Strength. In Rowell, R.M.

(ed). Handbook of Wood Chemistry and Wood Composites. CRC Press. Florida, USA.

Yahya, A.Z., & Weinland, G. (1995). A note on *Azadirachta excelsa*: a promising indigenous plantation species? Journal of Tropical Forest Science, 7(4), 672–676.

Yahya, A.Z., & Mahat, M.N. (1996). *Azadirachta excelsa*: growth performance and prospects as an indigenous plantation species. Proceedings of Forestry and Forest Products Research Conference. October 3–4, 1995, Kuala Lumpur.

Yahya, A.Z., & Mahat, M.N. (1998). The size of final crop trees of plantation grown *Azadirachta excelsa*. Journal of Tropical Forest Science, 10(3), 413–416.

Yahya, A.Z., & Mahat, M.N. (2002). Sentang. In Krishnapillay, B (ed). A manual for forest plantation establishment in Malaysia. Malayan Forest Records No. 45. Forest Research Institute Malaysia, Kuala Lumpur, Malaysia.

Zakaria, A.M., Jamaludin, M.A., Zakaria, M.Z., Hassan, R., & Bahari, S.A. Effect of incorporating different types of Sentang tree waste particle on the thermal stability of Wood Polymer Composite (WPC). IOP Conference Series: Earth and Environmental Science, 951, 012077.

Zerges, R.V., & Newman, R.D. (1980). Kraft pulp and paper properties of Populus clones under short-rotation intensive culture. Tappi, 63(7), 91–94.

Zhang, S.Y., Nepveu, G., & Owoundi, R.E. (1994). Intratree and intertree variation in selected wood quality characteristics of European oak (*Quercus petraea* and *Quercus robur*). Canadian Journal of Forest Research, 24(9), 1818–1823.

Zhang, S.Y. (1995). Effect of growth rate on wood specific gravity and selected mechanical properties in individual species from distinct wood categories. Wood Science and Technology, 29(6), 451–465.

Zhang, D., & Stanturf, J. A. (2008). Forest plantations. Encyclopedia of Ecology, 5 vols. pp. 1673–1680.

Zhong, B., Lv, C., & Qin, W. (2017). Effectiveness of the botanical insecticide azadirachtin against *Tirathaba rufivena* (Lepidoptera: Pyralidae). Florida Entomologist, 100(2), 215–218.

Zitting, A., Paajanen, A., Rautkari, L., & Penttilä, P. A. (2021). Deswelling of microfibril bundles in drying wood studied by small-angle neutron scattering and molecular dynamics. Cellulose, 28(17), 10765–10776.

Zobel, B.J., & van Buijtenen, J.P. (1989). Wood Variation: Its Causes and Control. Springer-Verlag, Berlin, Germany.

Zobel, B.J., & Jett, J.B. (1995). The importance of wood density (specific gravity) and its component parts. In Genetics of Wood Production. Springer, Berlin, Heidelberg.

Zobel, B.J., & Sprague, J.R. (1998). General concepts of juvenile wood. In Juvenile Wood in Forest Trees. Springer, Berlin, Heidelberg.

APPENDIX

Appendix A. Schultz solutions.

A 50 ml solution of nitric acid (70%) was mixed with 50 ml distilled water. A 6 g potassium chlorate was dissolved in 100 ml nitrate acid solution (35%).

Appendix B. Inventory data of the sample trees.

No.	Circumference (mm)	DBH (mm)
1.	1220	388
2.	1740	554
3.	1180	376
4.	1200	382
5.	1150	366
6.	1970	627
7.	860	274
8.	960	306
9.	870	277
10.	1090	347
11.	1030	328
12.	1100	350
13.	850	271
14.	1390	442
15.	1280	407
16.	1520	484
17.	1270	404
18.	1530	487
19.	1120	357
20.	1260	401
21.	1440	458
22.	1220	388
23.	15400	490
24.	1180	376
25.	1060	337
26.	1120	357
27.	1220	388
28.	1210	385
29.	1200	382
30.	1050	334
	Average	390
	SD	80

Appendix C. Fiber dimensions.

Tree categorize	Longitudinal position	Distance from the pith (mm)	Fiber dimensions (µm)			
			Length		Diameter	
			Average	SD	Average	SD
Slow-growth tree	Bottom	0–20	799	172	15	3
		20–40	703	132	16	2
		40–60	739	177	15	2
		60–80	718	140	12	2
		80–100	782	120	13	2
		100–120	799	120	15	2
	DBH	0–20	908	293	18.9	5
		20–40	841	208	14.7	3
		40–60	846	174	15.6	4
		60–80	825	130	14.5	3
		80–100	830	150	17.7	4
		100–120	969	210	19.3	4
	Middle	0–20	919	117	20.1	3
		20–40	840	178	18.8	3
		40–60	809	162	19.9	4
		60–80	866	180	18.1	4
		80–100	860	220	18.9	3
	Top	0–20	838	179	17.4	3
		20–40	905	188	17.6	3
		40–60	856	157	15.7	3
Average-growth tree	Bottom	0–20	1052	211	23.3	4
		20–40	1153	248	26.7	5
		40–60	1067	260	24.4	4
		60–80	1019	310	23.0	5
		80–100	808	150	18.8	2
		100–120	826	130	15.2	3
	DBH	0–20	883	262	20.1	4
		20–40	711	189	17.7	3
		40–60	779	167	17.9	3

		60–80	748	130	17.0	3
		80–100	831	160	18.0	3
		100–120	856	160	17.7	3
	Middle	0–20	1147	226	26.2	4
		20–40	1177	242	27.1	6
		40–60	1173	217	26.9	6
		60–80	998	270	24.9	6
		80–100	1088	260	25.2	5
		100–120	1127	300	24.5	4
		120–140	1117	220	26.3	4
	Top	0–20	845	297	18.8	5
		20–40	847	188	20.6	4
		40–60	963	193	21.3	4
	Bottom	0-20	1022	206	19.8	3
		20–40	1001	208	21.5	4
		40–60	775	222	18.5	3
		60–80	864	210	19.7	4
		80–100	825	150	19.9	3
		100–120	902	200	18.8	3
		120–140	881	250	18.5	4
		140–160	926	240	19.7	4
		160–180	795	210	19.2	4
Fast-growth tree	DBH	0–20	1012	364	27.8	8
		20–40	1148	286	22.8	5
		40–60	1021	333	21.9	7
		60–80	986	300	24.8	8
		80–100	877	200	20.7	5
		100–120	988	330	20.5	7
		120–140	1097	220	26.4	8
		140–160	1094	330	25.3	8
		160–180	1155	270	29.7	6
	Middle	0–20	707	143	15.0	3
		20–40	799	246	17.8	6
		40–60	758	170	15.9	4

	60–80	833	140	20.5	4
	80–100	828	130	16.4	3
	100–120	863	130	17.2	3
	120–140	893	160	18.2	5
Top	0–20	872	288	20.0	5
	20–40	908	330	21.3	6
	40–60	888	157	21.2	5
	60–80	890	210	18.8	4
	80–100	899	190	20.4	5
	100–120	1175	210	25.9	4
	120–140	997	240	23.0	5
	140–160	921	230	17.0	3

Appendix D. Vessel element dimensions.

Tree categorize	Longitudinal position	Distance from the pith (mm)	Vessel element dimensions (µm)			
			Length		Diameter	
			Average	SD	Average	SD
Slow-growth tree	Bottom	0–20	618	108	299	34
		20–40	523	130	323	70
		40–60	729	155	429	88
		60–80	634	146	357	84
		80–100	635	146	393	91
		100–120	707	165	450	76
	DBH	0–20	509	115	295	62
		20–40	602	99	318	46
		40–60	588	149	339	61
		60–80	603	120	470	74
		80–100	665	172	468	89
		100–120	571	138	461	71
	Middle	0–20	526	90	261	41
		20–40	655	126	348	53
		40–60	669	164	474	57
		60–80	602	109	499	95
		80–100	675	182	492	115
	Top	0–20	559	128	326	72
		20–40	683	125	362	53
		40–60	611	164	437	63
Average-growth tree	Bottom	0–20	555	127	213	30
		20–40	565	132	191	27
		40–60	497	146	193	41
		60–80	536	132	296	47
		80–100	596	146	391	80
		100–120	664	168	432	87
	DBH	0–20	524	95	222	44
		20–40	544	103	250	42
		40–60	607	99	372	64

		60–80	613	152	368	79
		80–100	563	142	377	98
		100–120	573	142	358	110
	Middle	0–20	553	129	266	53
		20–40	592	126	282	44
		40–60	617	130	384	67
		60–80	578	176	391	89
		80–100	568	139	356	73
		100–120	609	147	430	96
		120–140	625	162	432	110
	Top	0–20	519	100	291	39
		20–40	607	124	356	64
		40–60	572	134	377	82
	Bottom	0-20	503	103	174	39
		20–40	475	129	262	58
		40–60	560	142	334	107
		60–80	591	133	424	91
		80–100	622	108	361	124
		100–120	624	144	509	100
		120–140	614	170	449	100
		140–160	626	148	454	140
		160–180	600	180	404	120
Fast-growth tree	DBH	0–20	498	169	261	90
		20–40	555	100	355	65
		40–60	547	139	383	120
		60–80	623	173	371	86
		80–100	615	174	429	117
		100–120	641	125	438	91
		120–140	518	211	359	119
		140–160	581	131	464	134
		160–180	504	162	313	53
	Middle	0–20	488	186	261	101
		20–40	516	177	342	121
		40–60	488	187	319	105

	60–80	525	214	412	162
	80–100	410	206	344	159
	100–120	523	220	431	193
	120–140	591	205	445	169
Top	0–20	463	211	231	107
	20–40	573	116	368	59
	40–60	603	138	423	91
	60–80	500	204	322	130
	80–100	440	108	335	89
	100–120	623	168	363	100
	120–140	582	167	402	132
	140–160	529	197	425	173

Appendix E. The SEM images of the cross-section at breast height.

Tree categorize	Near the pith	Near the bark
Slow-growth tree	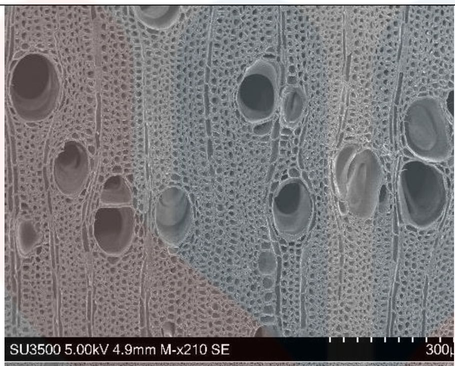	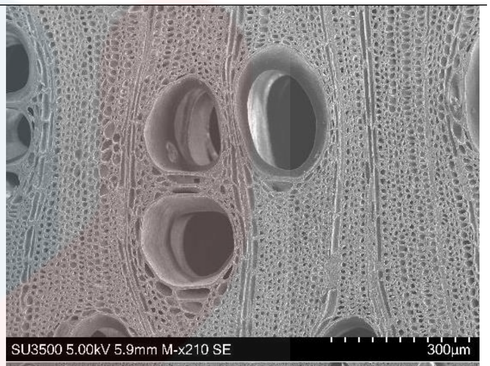
Average-growth tree	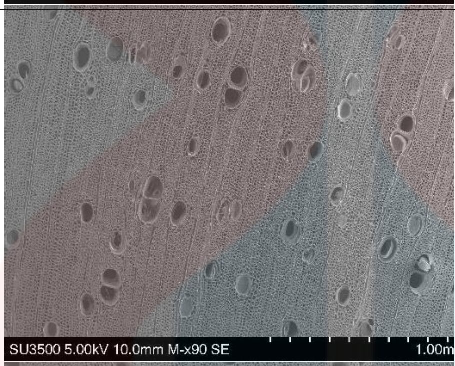	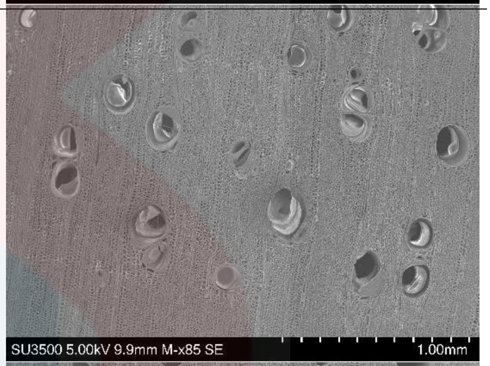
Fast-growth tree	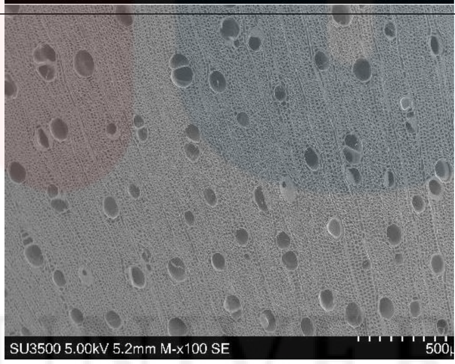	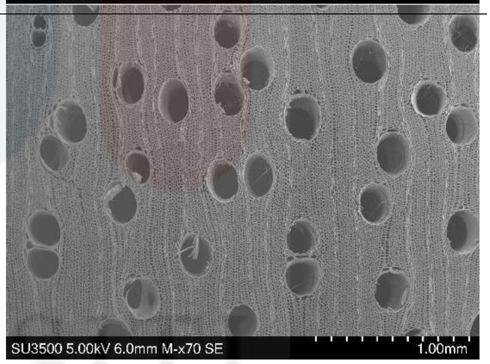

Appendix F. The relationship between shrinkage and MC.

Tree categorize	Longitudinal Position	Distance from the pith (mm)	Tangential		Radial		Longitudinal	
			Function	R^2	Function	R^2	Function	R^2
Slow-growth tree	Bottom	0–20	$y = 23.444e^{-0.145x}$	0.87	$y = 23.044e^{-0.198x}$	0.81	$y = 3.1707e^{-0.167x}$	0.69
		20–40	$y = 16.136e^{-0.136x}$	0.93	$y = 17.638e^{-0.179x}$	0.88	$y = 1.8003e^{-0.081x}$	0.93
		40–60	$y = 13.214e^{-0.108x}$	0.93	$y = 7.8129e^{-0.112x}$	0.95	$y = 1.3383e^{-0.072x}$	0.88
		60–80	$y = 8.5584e^{-0.074x}$	0.91	$y = 8.9355e^{-0.141x}$	0.93	$y = 2.818e^{-0.133x}$	0.79
		80–100	$y = 18.02e^{-0.153x}$	0.92	$y = 11.024e^{-0.158x}$	0.92	$y = 2.0014e^{-0.098x}$	0.88
		100–120	$y = 11.565e^{-0.121x}$	0.94	$y = 12.676e^{-0.165x}$	0.93	$y = 3.0378e^{-0.149x}$	0.79
		120–140	$y = 18.243e^{-0.143x}$	0.92	$y = 16.429e^{-0.184x}$	0.89	$y = 4.0908e^{-0.164x}$	0.75
	Breast height	0–20	-	-	-	-	-	-
		20–40	$y = 6.7401e^{-0.08x}$	0.92	$y = 4.0218e^{-0.077x}$	0.94	$y = 1.6293e^{-0.067x}$	0.93
		40–60	$y = 8.7064e^{-0.088x}$	0.94	$y = 7.3841e^{-0.117x}$	0.93	$y = 4.9824e^{-0.173x}$	0.89
		60–80	$y = 8.4303e^{-0.085x}$	0.93	$y = 8.3928e^{-0.133x}$	0.98	$y = 4.7192e^{-0.162x}$	0.78
		80–100	$y = 7.9155e^{-0.089x}$	0.94	$y = 8.4591e^{-0.121x}$	0.96	$y = 3.6226e^{-0.16x}$	0.84
		100–120	$y = 13.67e^{-0.137x}$	0.94	$y = 18.568e^{-0.193x}$	0.91	$y = 6.514e^{-0.205x}$	0.68
	Middle	0–20	-	-	-	-	-	-
		20–40	$y = 18.962e^{-0.153x}$	0.91	$y = 12.267e^{-0.156x}$	0.94	$y = 2.3217e^{-0.101x}$	0.72
		40–60	$y = 9.4478e^{-0.092x}$	0.94	$y = 7.9316e^{-0.115x}$	0.95	$y = 3.3781e^{-0.178x}$	0.80

		60–80	$y = 9.5388e^{-0.091x}$	0.94	$y = 7.4406e^{-0.12x}$	0.96	$y = 1.8489e^{-0.112x}$	0.92
		80–100	$y = 9.4779e^{-0.091x}$	0.93	$y = 8.462e^{-0.129x}$	0.94	$y = 4.2714e^{-0.197x}$	0.69
		100–120	$y = 11.384e^{-0.096x}$	0.93	$y = 7.5477e^{-0.12x}$	0.95	$y = 1.7075e^{-0.095x}$	0.81
	Top	0–20	-	-	-	-	-	-
		20–40	$y = 12.313e^{-0.132x}$	0.92	$y = 17.399e^{-0.194x}$	0.92	$y = 3.9192e^{-0.195x}$	0.75
		40–60	$y = 9.479e^{-0.108x}$	0.95	$y = 14.873e^{-0.169x}$	0.91	$y = 5.6644e^{-0.211x}$	0.77
		60–80	$y = 16.419e^{-0.138x}$	0.89	$y = 20.46e^{-0.202x}$	0.80	$y = 3.2571e^{-0.17x}$	0.68
Average-growth tree	Bottom	0–20	-	-	-	-	-	-
		20–40	$y = 16.181e^{-0.098x}$	0.93	$y = 9.5794e^{-0.118x}$	0.87	$y = 0.9797e^{-0.053x}$	0.76
		40–60	$y = 11.331e^{-0.088x}$	0.96	$y = 13.785e^{-0.152x}$	0.89	$y = 1.0345e^{-0.039x}$	0.83
		60–80	$y = 7.9985e^{-0.067x}$	0.92	$y = 10.463e^{-0.141x}$	0.96	$y = 1.498e^{-0.085x}$	0.95
		80–100	-	-	-	-	-	-
		100–120	$y = 8.2767e^{-0.079x}$	0.92	$y = 16.61e^{-0.179x}$	0.86	$y = 1.8201e^{-0.113x}$	0.85
		120–140	$y = 22.031e^{-0.19x}$	0.90	$y = 25.098e^{-0.217x}$	0.85	$y = 6.6399e^{-0.203x}$	0.80
	Breast height	0–20	-	-	-	-	-	-
		20–40	$y = 8.9351e^{-0.081x}$	0.94	$y = 8.4556e^{-0.135x}$	0.97	$y = 1.6833e^{-0.106x}$	0.93
		40–60	$y = 12.425e^{-0.101x}$	0.87	$y = 5.6195e^{-0.116x}$	0.96	$y = 1.612e^{-0.099x}$	0.89
		60–80	$y = 6.5767e^{-0.074x}$	0.88	$y = 5.8815e^{-0.114x}$	0.97	$y = 1.5695e^{-0.057x}$	0.93
		80–100	$y = 11.171e^{-0.106x}$	0.94	$y = 22.164e^{-0.203x}$	0.84	$y = 1.3801e^{-0.054x}$	0.94
		100–120	$y = 14.424e^{-0.142x}$	0.91	$y = 10.924e^{-0.16x}$	0.94	$y = 5.1345e^{-0.18x}$	0.91

		120–140	$y = 22.619e^{-0.154x}$	0.89	$y = 10.762e^{-0.146x}$	0.88	$y = 5.3301e^{-0.172x}$	0.85
	Middle	0–20	-	-	-	-	-	-
		20–40	$y = 11.822e^{-0.12x}$	0.93	$y = 13.891e^{-0.173x}$	0.90	$y = 3.1216e^{-0.135x}$	0.87
		40–60	$y = 16.988e^{-0.138x}$	0.93	$y = 12.375e^{-0.164x}$	0.89	$y = 1.8586e^{-0.084x}$	0.92
		60–80	$y = 29.67e^{-0.189x}$	0.84	$y = 10.084e^{-0.155x}$	0.90	$y = 3.3931e^{-0.13x}$	0.69
		80–100	$y = 10.106e^{-0.113x}$	0.95	$y = 7.5951e^{-0.134x}$	0.97	$y = 2.4131e^{-0.11x}$	0.94
		100–120	$y = 11.393e^{-0.117x}$	0.94	$y = 7.4149e^{-0.125x}$	0.97	$y = 2.9222e^{-0.114x}$	0.87
		120–140	$y = 14.166e^{-0.12x}$	0.94	$y = 7.7391e^{-0.124x}$	0.94	$y = 2.0827e^{-0.084x}$	0.80
		140–160	$y = 23.081e^{-0.156x}$	0.87	$y = 14.243e^{-0.173x}$	0.90	$y = 2.5651e^{-0.119x}$	0.81
	Top	0–20	-	-	-	-	-	-
		20–40	$y = 49.253e^{-0.243x}$	0.81	$y = 26.324e^{-0.228x}$	0.82	$y = 2.5737e^{-0.125x}$	0.81
		40–60	$y = 30.627e^{-0.2x}$	0.81	$y = 17.001e^{-0.188x}$	0.85	$y = 2.4723e^{-0.118x}$	0.81
		60–80	$y = 26.486e^{-0.174x}$	0.87	$y = 10.563e^{-0.149x}$	0.88	$y = 5.0796e^{-0.188x}$	0.76
Fast-growth tree	Bottom	0-20	-	-	-	-	-	-
		20–40	$y = 8.6245e^{-0.079x}$	0.93	$y = 6.277e^{-0.099x}$	0.92	$y = 1.3638e^{-0.04x}$	0.73
		40–60	$y = 13.554e^{-0.108x}$	0.94	$y = 6.3585e^{-0.096x}$	0.89	$y = 1.634e^{-0.08x}$	0.89
		60–80	$y = 10.169e^{-0.082x}$	0.94	$y = 6.0729e^{-0.091x}$	0.92	$y = 1.4747e^{-0.059x}$	0.90
		80–100	$y = 16.072e^{-0.133x}$	0.92	$y = 7.1121e^{-0.115x}$	0.94	$y = 1.6079e^{-0.063x}$	0.93
		100–120	-	-	-	-	-	-
		120–140	-	-	-	-	-	-

	140–160	$y = 5.7712e^{-0.054x}$	0.80	$y = 4.7528e^{-0.065x}$	0.85	$y = 1.4073e^{-0.06x}$	0.80
	160–180	$y = 7.578e^{-0.05x}$	0.88	$y = 6.498e^{-0.091x}$	0.92	$y = 1.4198e^{-0.05x}$	0.85
	180–200	$y = 13.29e^{-0.077x}$	0.95	$y = 6.4329e^{-0.08x}$	0.88	$y = 1.9376e^{-0.066x}$	0.78
Breast height	0–20	-	-	-	-	-	-
	20–40	-	-	-	-	-	-
	40–60	$y = 7.6673e^{-0.062x}$	0.89	$y = 5.3666e^{-0.075x}$	0.91	$y = 1.6632e^{-0.055x}$	0.81
	60–80	$y = 7.8076e^{-0.063x}$	0.91	$y = 7.0044e^{-0.093x}$	0.95	$y = 2.326e^{-0.067x}$	0.72
	80–100	$y = 6.7348e^{-0.037x}$	0.81	$y = 8.372e^{-0.104x}$	0.96	$y = 1.9379e^{-0.05x}$	0.91
	100–120	$y = 6.5949e^{-0.055x}$	0.88	$y = 5.8449e^{-0.075x}$	0.96	$y = 1.442e^{-0.044x}$	0.86
	120–140	-	-	-	-	-	-
	140–160	$y = 8.7297e^{-0.085x}$	0.93	$y = 5.0147e^{-0.059x}$	0.87	$y = 2.3312e^{-0.072x}$	0.94
	160–180	$y = 11.224e^{-0.053x}$	0.92	$y = 4.0337e^{-0.045x}$	0.87	$y = 1.4998e^{-0.05x}$	0.89
	180–200	$y = 9.3301e^{-0.058x}$	0.94	$y = 6.3724e^{-0.083x}$	0.94	$y = 1.8062e^{-0.046x}$	0.85
Middle	0–20	-	-	-	-	-	-
	20–40	-	-	-	-	-	-
	40–60	$y = 11.009e^{-0.121x}$	0.92	$y = 5.0578e^{-0.104x}$	0.92	$y = 2.3326e^{-0.088x}$	0.81
	60–80	$y = 9.5763e^{-0.073x}$	0.95	$y = 10.257e^{-0.105x}$	0.95	$y = 4.6177e^{-0.109x}$	0.83
	80–100	$y = 8.8745e^{-0.077x}$	0.91	$y = 7.3187e^{-0.074x}$	0.95	$y = 1.5517e^{-0.056x}$	0.90
	100–120	$y = 12.4e^{-0.062x}$	0.86	$y = 6.3577e^{-0.044x}$	0.87	$y = 1.3819e^{-0.046x}$	0.89
	120–140	$y = 8.4948e^{-0.049x}$	0.90	$y = 9.0967e^{-0.084x}$	0.87	$y = 1.477e^{-0.051x}$	0.89

	140–160	$y = 14.673e^{-0.071x}$	0.91	$y = 6.8206e^{-0.041x}$	0.84	$y = 1.5595e^{-0.044x}$	0.87
	160–180	$y = 9.7697e^{-0.049x}$	0.92	$y = 6.9671e^{-0.071x}$	0.96	$y = 1.5551e^{-0.068x}$	0.87
Top	0–20	-	-	-	-	-	-
	20–40	-	-	-	-	-	-
	40–60	$y = 7.8996e^{-0.089x}$	0.94	$y = 5.0827e^{-0.076x}$	0.94	$y = 1.4883e^{-0.053x}$	0.92
	60–80	$y = 6.9503e^{-0.077x}$	0.88	$y = 6.8126e^{-0.098x}$	0.86	$y = 1.6307e^{-0.072x}$	0.84
	80–100	$y = 7.0063e^{-0.071x}$	0.90	$y = 6.2964e^{-0.096x}$	0.93	$y = 1.1779e^{-0.042x}$	0.86
	100–120	$y = 9.0724e^{-0.082x}$	0.95	$y = 6.9795e^{-0.089x}$	0.90	$y = 2.1156e^{-0.094x}$	0.96
	120–140	$y = 10.815e^{-0.098x}$	0.96	$y = 7.7732e^{-0.107x}$	0.96	$y = 1.7161e^{-0.077x}$	0.95

Appendix G. Bending properties.

Tree categorize	Longitudinal Position	Distance from the pith (mm)	Bending properties (N/mm²)			
			MOR		MOE	
			Average	SD	Average	SD
Slow-growth tree	Bottom	0–20	67.64	2.80	7236	684
		20–40	77.26	4.84	6478	1123
		40–60	94.54	8.91	9746	1590
		60–80	93.99	9.93	9563	1757
		80–100	95.80	6.44	9630	727
		100–120	107.19	1.75	9905	545
		120–140	104.47	5.18	10069	681
	DBH	0–20	62.19	16.58	5959	1464
		20–40	82.11	11.88	7259	1174
		40–60	95.21	4.78	9359	975
		60–80	95.20	4.15	9558	719
		80–100	96.30	11.29	9158	1287
		100–120	93.18	7.76	8659	618
	Middle	0–20	45.00	18.16	4739	1844
		20–40	76.73	5.66	8830	327
		40–60	85.50	6.46	10080	97
		60–80	92.41	8.86	9913	1013
		80–100	97.50	12.29	10085	1780
		100–120	91.68	11.56	9124	1623
	Top	0–20	48.03	19.02	5778	2764
		20–40	79.91	0.54	10448	657
		40–60	83.51	4.32	10516	1553
		60–80	94.67	3.21	10488	1182
Average-growth tree	Bottom	0–20	57.56	5.88	4852	686
		20–40	56.05	7.21	4599	827
		40–60	59.00	14.18	4414	1018
		60–80	91.91	5.88	8012	1864
		80–100	73.71	17.67	6552	2627
		100–120	90.86	4.34	9870	73

		120–140	98.16	4.56	9936	812
	DBH	0–20	60.56	14.57	6678	2312
		20–40	84.99	1.18	8466	593
		40–60	81.96	0.94	7576	630
		60–80	94.39	8.84	9253	967
		80–100	97.34	1.39	9999	333
		100–120	93.22	5.44	9254	670
		120–140	92.57	6.39	10019	461
	Middle	0–20	48.45	22.02	4656	2480
		20–40	82.41	4.95	7957	725
		40–60	87.88	5.50	8000	1000
		60–80	84.61	1.31	8066	406
		80–100	84.74	9.51	7641	612
		100–120	94.17	3.87	9118	508
		120–140	88.15	2.58	8821	439
		140–160	83.07	5.03	8376	995
	Top	0–20	90.01	29.80	8118	2730
		20–40	113.15	4.58	9612	638
		40–60	96.17	9.45	8960	1648
		60–80	109.55	5.13	10328	499
Fast-growth tree	Bottom	0-20	66.35	6.15	5539	812
		20–40	71.86	1.87	7024	228
		40–60	78.25	8.04	7144	375
		60–80	67.01	20.14	6641	2012
		80–100	73.57	2.60	7272	574
		100–120	71.61	10.15	6307	2285
		120–140	80.39	22.08	7645	2257
		140–160	96.70	2.30	10720	350
		160–180	63.57	7.25	6524	1715
		180–200	71.57	8.20	8362	1207
	DBH	0–20	69.14	5.55	6985	114
		20–40	74.56	3.03	7264	1062
		40–60	76.84	4.46	9063	143
		60–80	74.16	9.93	7983	1016

	80–100	75.42	9.15	8327	785
	100–120	69.35	11.78	8179	1308
	120–140	86.84	4.25	8679	703
	140–160	84.82	9.28	8579	435
	160–180	82.24	7.66	9554	790
	180–200	85.21	9.62	9671	1881
Middle	0–20	38.94	3.07	5224	1496
	20–40	71.44	3.50	8966	648
	40–60	70.71	11.46	8721	584
	60–80	64.78	0.88	8507	743
	80–100	89.46	9.59	8789	956
	100–120	74.49	5.09	8890	1093
	120–140	84.40	18.82	8015	1849
	140–160	80.36	2.98	9004	419
	160–180	77.72	6.50	8378	607
Top	0–20	69.09	-	6728	-
	20–40	99.40	5.02	10291	220
	40–60	116.86	2.94	10878	166
	60–80	102.10	3.18	9933	494
	80–100	105.97	9.77	11342	874
	100–120	94.12	10.42	8062	962
	120–140	95.97	8.34	10134	1200